Incorporation of microalgae (*Nannochloropsis oceanica*) into plant-based fishcake analogue: physical property characterisation and *in vitro* digestion analysis

Lin Zhao [a], Hui Mei Khang [a], Juan Du [a *]

[a]*Food, Chemical and Biotechnology Cluster, Singapore Institute of Technology, 10 Dover Drive, Singapore 138683, Singapore*

Contact information for corresponding author (*)

Juan Du, Ph.D.

Associate Professor

Email: du.juan@singaporetech.edu.sg

Abstract

This study examined how incorporating microalgae into plant-based fishcake (PFC) analogue affected its physical properties and *in vitro* digestive profiles. PFCs were prepared using pea protein isolate blended with varying amounts of defatted *Nannochloropsis oceanica* biomass. Increasing the concentration of *N. oceanica* (up to 30%) progressively influenced the texture and rheological properties of PFC: the hardness and gel strength of PFC significantly increased, while springiness, expressible moisture and oil content decreased, making PFC more similar to the surimi-based fishcake. *In vitro* protein digestibility of PFCs varied with the concentration of *N. oceanica*: from 59.8% in the control PFC (without *N. oceanica*) increased to 74.9% with 10% *N. oceanica*, but only to 70.1% with 30% *N. oceanica*, which highlighted the role of microalgae concentration on the PFC's digestive profile. Furthermore, the release of metabolites in the PFC samples after *in vitro* digestion was evaluated using nuclear magnetic resonance (NMR) spectroscopy. The results showed that the digesta of PFC with 30% *N. oceanica* had reduced levels of most amino acids and linoleic acid, which might have ripple effects on the associated amino acid and fatty acid metabolisms in the human body upon consumption. Overall, the combination of pea proteins and *N. oceanica* biomass had the potential to contribute to the development of innovative plant-based seafood alternatives with modified physical properties and unique digestive characteristics. This study also provided valuable insights into the bioavailability of nutrients from *N. oceanica*-incorporated PFC, laying the foundation for their further launch on the market.

Keywords: Plant-based seafood analogue; Pea protein isolate; Texture; Rheological properties; Food metabolomics; Microstructure

1. Introduction

Surimi-based products such as fishballs and fishcakes are highly popular and consumed extensively in East and Southeast Asia due to their nutritional value (high protein, low fat) and unique texture (Shamasundar, 2023). However, concerns regarding overfishing and increasing people's environmental awareness have led to a growing demand for plant-based fish alternatives. As per a report released by Allied Market Research (2022), the worldwide market for plant-based seafood analogues reached a valuation of $42.1 million in 2021, and this market is expected to experience significant growth over the next decade, with a projected increase to $1.3 billion by 2031.

Although legumes (e.g., soybean, pea, and chickpea) and cereals (e.g., wheat, rice, and barley) have been the primary sources of plant proteins used in the production of plant-based meat/seafood analogues at present (Kumar et al., 2022), microalgae, which serve as another promising source of plant-based protein, have been gaining increasing attention as potential protein supplements in the food industry (Caporgno & Mathys, 2018). Unlike other plant-based protein sources, microalgae-based proteins exhibit remarkable sustainability in food production, as microalgae can be cultivated on non-arable land and require minimal freshwater consumption (Wang, Tibbetts, & McGinn, 2021). Additionally, they have high-quality protein profiles with well-balanced amino acid compositions that align with human nutritional needs (Becker, 2007). Out of the thousands of microalgae species available, *Nannochloropsis* sp. stands out as a relatively "novel" microalgae and its exploration as a viable food source for human consumption has not been extensively pursued thus far (Hernández-López et al., 2021).

The inclusion of *Nannochloropsis* as a novel food source is further supported by its notable protein content, ranging from 14.5% to 47.0% on a dry weight basis (Zanella & Vianello, 2020).

However, it should be noted that *Nannochloropsis* also possesses a higher lipid content (ranging from 37% to 60% on a dry weight basis) compared to other microalgae species (Paterson, Gómez-Cortés, de la Fuente, & Hernández-Ledesma, 2023), so the use of defatted *Nannochloropsis* biomass as a food ingredient could be more preferable, as it provides a concentrated source of protein while meeting the demand for low-fat food items that align with consumers' preference for a healthy diet (Gerde et al., 2013).

So far, a number of research has been conducted to explore the potential of combining microalgae with other plant-based proteins to develop novel meat alternatives, such as extruded meat analogues based on *Spirulina* biomass/lupin protein mixtures and *Auxenochlorella protothecoides* powder/soy protein concentrate blends (Caporgno et al., 2020; Palanisamy, Töpfl, Berger, & Hertel, 2019). These studies have highlighted the exceptional ability of microalgae in enhancing the nutritional characteristics and modifying the physicochemical properties of plant-based meat analogues when incorporated into their formulations.

However, to our knowledge, there have been no studies conducted on the utilisation of defatted *Nannochloropsis oceanica* biomass in conjunction with pea protein isolate for the production of plant-based fishcake (PFC) analogues. Pea protein has gained increasing popularity in the market due to its lower allergenic potential compared to proteins derived from wheat and soybean, as well as its favorable nutritional profile and functional properties (Asen & Aluko, 2022). As a result, pea protein was selected as the primary ingredient in this study for the development of PFC. On the other hand, while the fishy odor of *N. oceanica* may be considered undesirable in many food applications, it can be sought after for enhancing the flavour of PFC (Coleman et al., 2022).

Therefore, the objective of the current research was to develop a novel *N. oceanica*-enriched PFC using pea protein as the base ingredient, with comparable physical properties to traditional surimi-based fishcake (SFC) while offering enhanced nutritional functionality. Several physical properties, including texture, expressible moisture and oil content, and rheological behaviour, were examined and compared across different PFC groups with varying levels of *N. oceanica* incorporation. Additionally, the impact of *N. oceanica* on the metabolite release and nutritional quality of PFC was investigated through *in vitro* digestion modeling and nuclear magnetic resonance (NMR) spectroscopy. Finally, the microstructures of different PFC samples were examined using scanning electron microscopy (SEM) before and after *in vitro* digestion, providing visual evidence and support for the textural and digestibility characteristics of PFCs observed earlier. This study lays the groundwork for expanding the range of plant-based seafood analogues by incorporating microalgae as a supplement.

2. Materials and methods

2.1 Materials

The pea protein isolate (PPI, Radipure™ E8001G, Cargill Pte. Ltd. (Singapore)), defatted *Nannochloropsis oceanica* biomass (Wintershine Pte. Ltd. (Singapore)), microbial transglutaminase (mTG, Activa® TG-SR-MH, 25−57 U/g, Ajinomoto Pte. Ltd. (Singapore)), methylcellulose (Benecel™, Ashland Pte. Ltd. (Singapore)), and gellan gum (Kelcogel® MA-60, CP Kelco Pte. Ltd. (Singapore)) were kindly provided by the respective company. The remaining ingredients, i.e., salt, sugar, monosodium glutamate, white pepper, sunflower oil, and dextrose monohydrate were purchased from the local supermarket. Frozen fish surimi (*Itoyori*) was supplied by Ha Li Fa Pte. Ltd. (Singapore).

Following digestive enzymes were purchased from Sigma-Aldrich Pte. Ltd. (Singapore): α-amylase (EC 3. 2. 1. 1, isolated from porcine pancreas, with an activity of 12 U/mg), pepsin (EC 3. 4. 23. 1, isolated from porcine gastric mucosa, with an activity of 3940 U/mg), and pancreatin (EC 232. 468. 9, isolated from porcine pancreas, a combination of various digestive enzymes including amylase, trypsin, lipase, ribonuclease and protease, with a trypsin activity of 96.7 U/mg). Bile extract and other chemical reagents (analytical grade) used for *in vitro* digestion were also procured from the same company.

2.2 Proximate composition, heated water holding capacity (HWHC) and heated oil holding capacity (HOHC) of PPI and N. oceanica biomass

The proximate composition of PPI and *N. oceanica* biomass, which includes protein, moisture, carbohydrate, fat and ash, was assessed using the standard methods outlined in AOAC (2005), and the results are shown in the Supplementary (Table S1). Specifically, the evaluation of PPI and *N. oceanica*'s HWHC and HOHC was conducted following a modified version of a previous method by Nasrin, Noomhorm, & Anal (2015). These two properties were of interest as they were considered crucial in assessing the mouthfeel of our final PFC products. To perform the evaluation, a sample weighing 0.1 g was added to a pre-weighed centrifuge tube containing 10 mL of deionised water/sunflower oil. Complete dispersion of the sample was achieved by vigorous vortex mixing at the highest speed for 1 min. Subsequently, the tube was placed in a water bath at 95 °C for 30 min and promptly cooled in an ice bath. After centrifugation (Sartorius Centrisart® D-16C) at 4000×*g* at 25 °C for 25 min, the supernatant was decanted, and the tube with the remaining residues was re-weighed. The HWHC and HOHC values were then calculated using the following equation:

$$\text{HWHC/HOHC} = \frac{\text{Weight of residue (g)} - \text{Weight of dry sample (g)}}{\text{Weight of dry sample (g)}} \quad (1)$$

2.3 Sample preparation

Throughout our preliminary trials, we extensively explored various formulations for our PFC, with the primary aim of creating a PFC that closely emulated the properties of real surimi-based fishcake. Following a thorough evaluation of the overall appearance and initial texture (both visually and tactilely), we determined the specific concentration of ingredients and the details of PFC formulations with varying levels of *N. oceanica* addition can be found in Table S2. As shown, there were 4 kinds of PFCs in this study, i.e., PP + NO (10:0), (9:1), (8:2) and (7:3), with different ratios of PPI and *N. oceanica* in the PFC, respectively. In our initial trials, we observed that a microalgae concentration exceeding 30% resulted in an overly firm texture in our PFC. The texture was more akin to "fishbread" rather than the desired "fishcake", and the colour was darker than intended (data not shown). Therefore, we decided to incorporate *N. oceanica* biomass at varying levels: 0%, 10%, 20%, and 30% (set as the maximum concentration), substituting the corresponding percentage of PPI with a gradual increase in our PFC product, respectively. This allowed us to examine how these varying levels of microalgae impacted the PFC product.

The preparation process of PFC began by combining methylcellulose, seasoning and sunflower oil in a food processor (Philips HR7320/01). This mixture was blended first for 1 min at a low speed (Speed 1). Next, the remaining dry ingredients, including PPI and *N. oceanica* in different ratios, mTG, gellan gum and filler, were added and blended for an additional 1 min at a high speed (Speed 2). Cold ice water was then added, and the entire mixture was blended for the last 3 min at high speed (Speed 2). The resulting paste was manually shaped into a square using a mold measuring 4.5 × 4.5 cm. The molded paste underwent a two-step heating process to enhance its gelling properties. Initially, it was placed in a water bath at 45 °C for a 30-min setting.

Subsequently, it was cooked in boiling water for 10 min under high heat. Afterward, the samples were cooled in ice water for 15 min, followed by deep-frying in a fryer (Tefal FF2200) for 3 min at 180 °C.

On the other hand, a benchmark surimi-based fishcake (SFC) was prepared to serve as a point of reference for comparing and enhancing the PFC. The formulation of SFC was determined based on a previous study by Ran, Lou, Zheng, Gu, & Yang (2022), which consisted of surimi (88.5% w/w), salt (1.5% w/w), starch (5.0% w/w), and cold ice water (5.0% v/w). These ingredients were mixed and blended for 3 min using a food processor. The subsequent procedures including molding, setting, boiling, cooling, and frying were carried out in the same manner as the PFC samples. After frying, both PFC and SFC samples were placed on paper towels to drain excess oil for 5 min. Subsequently, they were cooled at room temperature for 30 min before undergoing further analysis. After cooling, the physical properties of PFC were immediately tested in accordance with the respective steps outlined in Section 2.4. The samples intended for *in vitro* digestion were packed in ziplock bags and stored in a refrigerator at 4 °C, with the digestion process commencing within 48 h. For the microstructure test, samples before and after *in vitro* digestion were stored in the freezer for a minimum of 48 h. Afterward, they were subjected to freeze-drying and tested as described in Section 2.8.

2.4 Physical property characterisation of PFC

2.4.1 Texture profile analysis

To analyse the texture profile, a Texture Analyser (TA.XT Plus, Stable Micro Systems, Surrey, UK) equipped with a flat-ended 36 mm aluminum cylinder probe (P/36R) was employed. Prior to analysis, the samples were prepared by removing the crust and cutting them into 1.5 cm

cubes. These cubes were put in ziplock bags and then pre-warmed in a water bath at 55 °C for 1 h to replicate the temperature at which consumers typically consume the product. During the analysis, the samples were compressed to 60% of their original height at a test speed of 1 mm/s, with a holding time of 5 s. Two textural parameters, specifically hardness and springiness, were measured and recorded (Abdol Rahim Yassin, Binte Abdul Halim, Taheri, Goh, & Du, 2023).

2.4.2 Expressible moisture and oil content

The determination of expressible moisture and oil content followed a modified version of a previously established method by Chaijan, Panpipat, & Benjakul (2010). Freshly cut PFC samples in the form of 1 cm cubes were used for the analysis. Initially, any moisture and oil present on the surface of the sample were removed by blotting with tissue paper, and the initial weight of the sample was recorded. Next, the sample was sandwiched between two pre-weighed filter papers (2 cm × 2 cm) and compressed using a standard weight (300 g) for a duration of 10 min. Subsequently, the two wet filter papers were weighed again and transferred to a drying oven (UN 55, Memmert, Germany) set at 105 °C for 24 h. The final dried weight of the filter papers was then recorded. The expressible moisture and oil content were calculated using the following equations:

$$\text{Expressible moisture (\%)} = \frac{W_1\,(\text{g}) - W_2\,(\text{g})}{\text{Initial weight of sample (g)}} \times 100\% \quad (2)$$

$$\text{Expressible oil (\%)} = \frac{W_2\,(\text{g}) - W_0\,(\text{g})}{\text{Initial weight of sample (g)}} \times 100\% \quad (3)$$

where W_0 is the original weight of filter papers before compression, W_1 is the wet weight of filter papers after compression, W_2 is the dried weight of filter papers after drying.

2.4.3 Rheological measurements

The rheological properties of PFC were evaluated using a rotational stress-controlled rheometer (MCR 302e, Anton Paar GmbH, Graz, Austria) equipped with a cross-hatched parallel plate measuring 25 mm in diameter. The PFC sample, with the crust removed, was sliced to a diameter of 25 mm and a thickness of 3 mm. An amplitude sweep test was initially conducted at 55 °C, which involved applying a constant frequency of 1 Hz and incrementally increasing the strain from 0.01% to 100% with 10 data points per decade. This test allowed for the determination of the linear viscoelastic (LVE) region for all samples, which aided in setting consistent strain and stress values for subsequent measurements (Ran, Lou, et al., 2022). Once the destroyed sample was substituted, a frequency sweep test was performed subsequently at the same temperature. The test covered a frequency range of 0.1 to 10 Hz, with a fixed strain amplitude of 0.1% within the LVE region (Taheri, Kashaninejad, Tamaddon, Du, & Jafari, 2023).

2.5 In vitro *digestion of PFC*

The experimental setup for *in vitro* digestion involved a three-phase model consisting of oral, gastric, and intestinal stages. The protocol used for this model was based on established references (Minekus et al., 2014; Zhao, Chen, Bi, & Du, 2023). To replicate the different digestive stages, specific electrolyte stock solutions were prepared following the composition described in Table S3, encompassing simulated salivary fluid (SSF), simulated gastric fluid (SGF), and simulated intestinal fluid (SIF). Before the digestion process, the PFC samples were manually minced to achieve uniform size among different groups, resulting in 2 mm × 1 mm × 1 mm cubes. The minced samples, weighing 5 g in each group, were transferred into a 50 mL centrifuge tube and pre-heated to 37 °C prior to digestion.

For the simulated oral digestion phase, a total of 5 mL of electrolyte solution was prepared. This solution consisted of 4 mL of α-amylase SSF solution with a final enzyme activity of 75 U/mL, 0.025 mL of $CaCl_2$ solution (0.3 mol/L), 0.965 mL of deionised water, and 0.01 mL of HCl (2 mol/L) to adjust the final pH value to 7.0. These components were thoroughly mixed and pre-warmed to 37 °C before being combined with 5 g of the samples. The mixture was then incubated at 37 °C for 2 min with shaking at 200 rpm.

For the simulated gastric digestion phase, a total of 10 mL of electrolyte solution was prepared. This solution comprised 8 mL of pepsin SGF solution with a final enzyme activity of 2000 U/mL, 0.005 mL of $CaCl_2$ solution (0.3 mol/L), 1.76 mL of deionised water, and 0.235 mL of HCl (2 mol/L) to correct the final pH value to 3.0. After warming the solution to 37 °C, the gastric solution was added to the products from the oral phase. The mixture was continually digested in a 37 °C water bath for 2 h with shaking at 200 rpm.

For the simulated intestinal digestion phase, a total of 20 mL of electrolyte solution was prepared. This solution contained 16 mL of pancreatin SIF solution with a final enzyme activity of 100 U/mL based on its trypsin activity, 0.04 mL of $CaCl_2$ solution (0.3 mol/L), 0.08 mL of amyloglucosidase, 3.81 mL of deionised water, and 0.07 mL of NaOH (2 mol/L) to change the final digesta pH value to 7.0. Additionally, 0.1768 g of bile was added to the solution, which required thorough mixing in a shaking water bath at 37 °C for 30 min to ensure complete bile solubilisation. Then, the mixture was combined with the products that had completed the gastric digestion phase, which continually underwent final 2-h digestion in a 37 °C water bath with shaking at 200 rpm. The completed products from the intestinal phase were promptly subjected to a 10-min heat treatment in a water bath set at 95 °C to deactivate the digestive enzymes and halt the digestion reaction.

To assess the degree of protein digestion, the *in vitro* protein digestibility of PFC was further evaluated. The Kjeldahl method was employed to determine the total protein content of PFC before digestion, as well as the protein content of the undigested PFC residues remaining after the intestinal phase. Both analyses were conducted following the protocol outlined in the AOAC (2005) standard. Furthermore, the release of metabolites such as amino acids and fatty acids from each group of PFC digests was discussed in the subsequent sections.

2.6 NMR spectroscopic analysis

After the digestion of each PFC sample, the resulting digesta was subjected to centrifugation at 10000×*g* for 5 min at 4 °C to remove undigested precipitates. The supernatants obtained were then filtered through a 0.22 μm membrane and subsequently freeze-dried for 5 days in preparation for NMR analysis. In parallel, the digestive enzymes utilised during the *in vitro* digestion process were individually dissolved in water at concentrations equal to those in the intestinal phase. This enabled the acquisition of their respective NMR spectral signals within the collected digesta spectra.

After freeze-drying, each sample weighing 30 mg was thoroughly mixed with 1 mL of deuterated water (D_2O, 99.9%) containing 0.01% sodium 3-trimethylsilyl [2,2,3,3-d_4] propionate (TSP, Sigma-Aldrich, USA). The mixture was then subjected to centrifugation at 4 °C for 10 min at a speed of 12000×*g*, as described by Zhao, Zhao, Wu, Lou, & Yang (2019). Following centrifugation, 600 μL of each supernatant was carefully transferred into a 5-mm (diameter) NMR tube for subsequent measurement and analysis.

All NMR experiments were carried out using an 800 MHz Bruker Avance Neo NMR spectrometer equipped with a Bruker TXI cryoprobe at a temperature of 298 K. The 1D ^{1}H spectra

were collected first using the standard NOESY setting (noesypr1d), and the specific parameters employed can be found in our previous study (Zhao et al., 2022). Additionally, to facilitate the identification of metabolic signal assignments, a 2D ^{1}H-^{13}C heteronuclear single quantum coherence (HSQC) spectrum was acquired and analysed for a representative sample, with 180 ppm ^{13}C spectra in F1 channel and 10 ppm ^{1}H spectra in F2 channel.

2.7 Spectral processing and analysis

The phase adjustment and baseline correction of each sample spectrum were initially performed using TopSpin 4.0.7 software (Bruker). Reference databases such as the Biological Magnetic Resonance Data Bank (http://www.bmrb.wisc.edu/) and the Human Metabolome Database (http://www.hmdb.ca/) were utilised cooperatively to aid in the identification of metabolites from the 2D ^{1}H-^{13}C NMR spectrum and 1D ^{1}H spectra. The peaks in the 1D ^{1}H spectra ranging from 0 to 10 ppm were normalised and integrated using MestReNova 9.0.1 (Mestreab Research SL, Santiago de Compostela, Spain), with reference to the TSP peak area located at 0 ppm. The normalised spectra were divided into region buckets with a width of 0.01 ppm. These region buckets were then separated, resulting in a binned dataset that was used for subsequent multivariate analysis.

The binned data were subjected to principal component analysis (PCA) using SIMCA14 (Umetrics, Sweden) to visualise the separation between datasets and identify the metabolites responsible for the separation. Euclidean distances were calculated among each group based on the obtained PCA score plots. Additionally, orthogonal projection to latent structure discriminant analysis (OPLS-DA) was employed to highlight the intergroup differences in metabolomic release profiles among different pairwise groups of PFCs. To identify the metabolites that their release

after *in vitro* digestion were significantly influenced by the addition of *N. oceanica*, the variable importance in projection (VIP) scores were analysed for each pairwise comparison (Ran, Yang, Chen, & Yang, 2022). Furthermore, metabolic enrichment analysis was performed by submitting the screened metabolites (VIP value > 1) to MetaboAnalyst 5.0 (https://www.metaboanalyst.ca/), with references to the Kyoto Encyclopedia of Genes and Genomes (KEGG) pathway database (https://www.genome.jp/kegg/pathway.html).

2.8 Microstructure test

The surface microstructures of SFC and PFC samples, both before and after *in vitro* digestion, were examined using scanning electron microscopy (SEM) (JSM IT800, Jeol Asia, Tokyo, Japan). The samples were freeze-dried and then dispersed onto a conductive adhesive tape that was affixed to an aluminum plate. A thin film coating of platinum was applied to the samples. The observations were conducted under a 10 kV accelerating voltage, and a magnification of 300× was used to visualise the surface morphology of each sample (Binte Abdul Halim et al., 2023).

2.9 Statistical analysis

Each experiment was independently conducted in triplicates. The results are expressed as mean values ± standard deviations. Statistical analysis was conducted using SPSS24 software (IBM Corp., Armonk, NY, USA). Duncan's multiple range test and one-way analysis of variance (ANOVA) with a significance level of $P < 0.05$ were applied to assess statistically significant differences among the different sample groups.

3. Results and discussion

3.1 N. oceanica effects on PFC physical properties

Fig. S1 displays the overall appearance and cutting profiles of SFC and PFCs. It was observed that SFC exhibited the highest whiteness compared to PFCs, while the colour of PFCs became progressively darker with the increasing concentrations of *N. oceanica* biomass. The cutting profiles revealed that the internal structure of SFC was the most compact, with evenly distributed small air pores. In contrast, the control PFC (PP + NO (10:0)) showed an uneven distribution of larger pores. As the level of *N. oceanica* increased, PFCs exhibited fewer and smaller pores, resulting in a denser and tighter texture. This phenomenon could be attributed to *N. oceanica* acting as a filler, filling the network gaps in the PPI-based gel system and reducing bubble formation during the fishcake-making process (Kazir & Livney, 2021). To gain a deeper understanding of how *N. oceanica* concentrations affect the physical properties of PFCs, additional investigations were conducted on their texture profiles, expressible moisture and oil contents, and rheological properties, which were discussed in detail below.

3.1.1 Texture profile analysis

As depicted in Fig. 1A, the hardness of SFC was notably higher than that of PFCs. This finding aligned with expectations since the myofibrillar proteins in surimi were observed to undergo various conformational changes, such as the transformation of α-helix secondary structures into β-sheets, as well as the development of intermolecular bonds like ionic bonds, hydrogen bonds, and disulfide bonds, throughout the process of heat-induced gelation (Yan et al., 2020). These changes played a significant role in the formation of robust thermal gels following the cooking stage. In the case of PFCs, the incorporation of *N. oceanica* at lower concentrations (10% and 20%) did not result in significant changes in hardness compared to the control group,

with all measurements around 11 N. However, when the concentration of *N. oceanica* reached 30%, the PP + NO (7:3) group exhibited a notable increase in hardness, albeit still lower than that of the SFC counterpart. Our findings agreed with a previous study conducted by Atitallah et al. (2019), in which microalgae-enriched canned fish burgers demonstrated improved textural characteristics in concentration-dependent pattern. The presence of microalgae components, such as fibres, proteins, polysaccharides, etc., was believed to play a significant role in modifying the hardness of food products, by facilitating the formation of intermolecular networks and bonded aggregates that enhance the texture of the final product (Wang et al., 2023). Therefore, the *N. oceanica*-induced aggregates formed during heat processing in our study could fill in the PPI-based network as fillers and improve the hardness of the PFC gel. However, insufficient concentration of *N. oceanica* could result in the filler not being enough to effectively enhance the gel hardness.

On the other hand, Fig. 1B illustrates the springiness of fishcake samples with various formulations. The results indicated that the control PFC and PFC fortified with 10% *N. oceanica* exhibited the highest springiness. However, as the concentration of *N. oceanica* increased, the springiness decreased in the PP + NO (8:2) and PP + NO (7:3) groups, while the SFC showed the lowest springiness. The presence of an adequate moisture content in food is believed to contribute to maintaining its springiness (Li et al., 2018). Therefore, the denser gel networks created by the *N. oceanica* incorporation could impede the entry of water molecules into our PFC gels, leading to a reduction in springiness of PFCs supplemented with higher amounts of *N. oceanica*. On the other hand, as springiness of food refers to how far it returns to its original shape after the deforming force is removed, the compact structure of SFC as stated above following the cooking

process might offer limited gaps within the structure for deformation, resulting in reduced springiness (Bourne, 2002).

3.1.2 Expressible moisture and oil content

The potential causes of the structural changes in PFC induced by microalgae could be attributed to variations in water absorption and lipid integration. To investigate this, the levels of expressible moisture and oil were analysed, and the findings are presented in Fig. 1CD. The results revealed a consistent decrease in both expressible moisture and oil contents as the concentration of *N. oceanica* in PFCs increased. These results aligned with the HWHC and HOHC findings obtained from our preliminary trials, wherein *N. oceanica* exhibited higher values for both properties (HWHC: 5.39 g/g; HOHC: 6.56 g/g, data not shown) compared to PPI (HWHC: 3.51 g/g; HOHC: 6.25 g/g, data not shown), suggesting in addition to proteins, other components in *N. oceanica* like fibres might also play a synergistic role in enhancing its ability to absorb water and lipids (Atitallah et al., 2019). Our results were consistent with one earlier research stating that the incorporation of microalgal biomass could considerably enhance the water holding capacity and oil holding capacity of food items (Chen, Tang, Shi, Zhou, & Fan, 2022). Therefore, a higher concentration of *N. oceanica* not only imparted elasticity to PFC, as mentioned earlier, but also amplified its juiciness by retaining more water and oil within the well-structured gel matrices induced by *N. oceanica*. This led to a mouthfeel resembling that of SFC, enhancing the overall sensory experience.

3.1.3 Rheological properties

Rheological amplitude and frequency sweeps were conducted to investigate the rheological properties of SFC and PFCs. In both tests, the storage modulus (G') of all samples was

approximately ten times greater than their loss modulus (G"), indicating a solid or gel-like structure. Consequently, only G' values are displayed in Fig. 2.

To determine the strain range in which the sample structure remained intact, oscillatory amplitude testing was performed first, defining the LVE region. As depicted in Fig. 2A, the LVE region threshold for SFC was approximately 2.52%, surpassing that of the control PFC, which was around 1.27%. This indicated that SFC exhibited greater structural strength, which aligned well with its higher hardness observed in Section 3.1.1. However, when compared to the control PFC, the LVE region limit in microalgae-incorporated PFCs all showed varying degrees of increase (3.18%, 1.59%, and 2.01% in PP + NO (9:1), PP + NO (8:2), and PP + NO (7:3) group, respectively), and the G' values of the microalgae-incorporated PFCs consistently increased with higher levels of *N. oceanica* biomass added, suggesting that the presence of *N. oceanica* significantly enhanced the structural strength of the PFC gel system (Fig. 2A). A similar observation was reported in a prior study, where the addition of *Spirulina platensis* improved the network structure of the soy protein isolate gels, resulting in concentration-dependent increases in G' values as well (Wang et al., 2023). Due to the potential damage caused by the ethanol-based lipid extraction treatment to the cell wall of *N. oceanica*, it was likely that intracellular components such as proteins and polysaccharides were released from the cells during fishcake making (Yang et al., 2015). These components might have contributed to filling the PPI hydrogel network and facilitating the formation of a uniform and compact network structure in our PFCs (Wang et al., 2023). Consequently, the incorporation of *N. oceanica* into PFCs, particularly at a higher concentration (30%), led to increased hardness and gel strength, which was in accordance with the TPA results mentioned earlier.

Additionally, the frequency dependence of SFC and PFCs at a 0.1% strain amplitude within the LVE region is illustrated in Fig. 2B. The mechanical spectra showed that G' values progressively increased across the frequency range for all groups. However, the *N. oceanica*-incorporated PFCs exhibited a more solid-like behavior with higher G' values compared to the control PFC, which aligned well with a previous study on the impact of microalgae addition on dough rheology (Graça, Fradinho, Sousa, & Raymundo, 2018). Based on the findings reported previously, the addition of *N. oceanica* in our study might strengthen the PFC gel structure by reinforcing the protein matrix and increasing the number of entanglement points between the molecular chains in the gel system (Graça et al., 2018; Wang et al., 2023). Our results indicated that introducing microalgae to PFC could result in stronger and more elastic gels, thereby enhancing the textural properties of PFC to closely resemble those of its SFC counterpart.

3.2 N. oceanica effects on in vitro *protein digestibility*

The typical way of assessing the bioavailability of dietary proteins is by measuring their digestibility, which can be served as an important indicator of our PFC's nutritional values. As shown in Fig. 3, there is a notable difference in the protein digestibility of real SFC versus control PFC during simulated gastrointestinal digestion, decreasing from 76.9% in SFC to 59.8% in control PFC at the end of intestinal digestion. The reason for this finding could be explained by the increased viscosity of simulated gastrointestinal fluids resulting from the addition of some thickeners (e.g., methylcellulose and gellan gum as shown in Table S2) used to make PFC more closely resemble SFC's texture in our study. The thickening of the gastrointestinal fluids could potentially hinder the interaction between protein and digestive enzymes, ultimately leading to a decrease in protein hydrolysis (Xie et al., 2022). Additionally, the differences in protein

digestibility between SFC and PFC might also be attributed to their distinct gel structures after undergoing heat treatments. Under heating conditions, SFC featured a homogeneous actomyosin gel network with fine and elastic structure, while PFC had a hybrid gel made up of a mixture of polysaccharides and proteins, where pea proteins existed as particles rather than serving as agents for gel formation (Shamasundar, 2023; Wang, Kim, Naik, Spicer, & Selomulya, 2023). The rigid and dense hybrid gel network formed in PFC could restrict the accessibility of proteolytic enzymes during digestion, resulting in decreased protein digestibility. Furthermore, the existence of remaining anti-nutritional factors (e.g., trypsin inhibitors, phytic acid, lectins, saponins, etc.) in control PFC even after processing could also contribute to its lower protein digestibility to some extent (Samtiya, Aluko, & Dhewa, 2020).

When incorporating 10% defatted *N. oceanica* biomass to PFC as a substitute for the PPI, a dramatical increase of digestibility (reaching 74.9%) was shown in the PP + NO (9:1) group, as compared to that of the control PFC (Fig. 3). A similar result was found by Neumann et al. (2018), in which the diet containing 5% *N. oceanica* biomass exhibited an observable protein digestibility of 89%, which was greater than the 83% observed in the control casein-based diet for mice. As the size of the *N. oceanica* biomass was considerably larger than that of the PPI and other food components in PFC, its inclusion could potentially reduce the clustering of pea protein particles and weaken the bonding between pea proteins and other PFC components. This might lead to an increase in the surface areas accessible to digestive enzymes, ultimately resulting in a higher extent of protein digestion.

However, with the increasing concentration of *N. oceanica*, a significant decrease of protein digestibility was observed in the PP + NO (7:3) group (falling to 70.1%), although still higher than that of control PFC (Fig. 3). Based on our observations, we found that the PFC digesta

from the PP + NO (7:3) group appeared to be more adhesive after undergoing *in vitro* digestion, in comparison to other PFC counterparts. This result was in line with a prior study that reported an increase in the viscosity of duodenum and jejunum contents in piglets fed with microalgae (Martins et al., 2022). Therefore, the elevated digesta viscosity in PFC containing higher concentration of *N. oceanica* might impede the access of digestive enzymes to their intended substrates, ultimately compromising the digestibility of nutrients. On the other hand, as the cell wall structure of our defatted *N. oceanica* could be weakened or disrupted during ethanol-based lipid extraction, it was possible that additional non-protein components, such as the indigestible non-starch polysaccharides and fibres, were released from the *N. oceanica* biomass in the PP + NO (7:3) group (Annamalai et al., 2021; Yang et al., 2015). These components could then act as blocking barriers to the proteolytic enzymes and limit enzyme−protein interactions, resulting in a decrease in the digestibility of protein as well. Furthermore, as stated in Section 3.1.1, the elevated firmness of PFC resulting from a higher concentration of *N. oceanica* incorporation might also be a factor contributing to the reduced digestibility. This is because firmer foods tend to break down more slowly and take longer time to soften during digestion, as previously documented (Bornhorst, Ferrua, & Singh, 2015).

3.3 Metabolite profiles after in vitro *digestion*

Our research is the initial endeavour to employ NMR-based metabolomics for unravelling the digestive properties of *N. oceanica*-incorporated plant-based fishcake analogue during *in vitro* digestion. The ^{1}H NMR spectra of metabolite extracts from SFC and PFC digesta are shown in Fig. 4A. Based on signals from 0.5 to 9.5 ppm, there were totally 29 metabolites identified in both SFC and PFC samples after *in vitro* digestion, encompassing a set of primary metabolites like

amino acids, fatty acids and sugars. In Table S4, a list of chemical shift assignments for each metabolite is presented in detail, which was accomplished by comparing and analysing the 1D ^{1}H and 2D $^{1}H–^{13}C$ NMR spectra obtained in our research with those from metabolic database.

Overall, the spectra displayed a significant resemblance in metabolic species across SFC's and all kinds of PFCs' digesta, albeit with different signal strength of certain individual metabolites (Fig. 4A). The region between 1.0 and 4.0 ppm of ^{1}H spectra was primarily associated with the majority of amino acids (except Phe, Trp, Tyr and His, whose characteristic peaks were located in the region of 6.5−8.5 ppm) and fatty acids (e.g. linolenic acid, oleic acid and palmitic acid), while the signals observed between 4.0−5.5 ppm were typically attributed to sugars (α-D-glucose, β-D-glucose, sucrose, etc.) (Zhao et al., 2019). Our findings were in accordance with the breakdown of the main ingredients in our samples under enzymatic hydrolysis, and were consistent with earlier research, which demonstrated similar metabolic compounds in cooked fish products (e.g., sea bass fillets) and plant-based seafood analogues (e.g., soy protein-based fishball) after *in vitro* digestion (Ran, Yang, et al., 2022; Vidal et al., 2016).

In order to initially visualise the changes in metabolite concentration among different groups of fishcakes, z-score transformed NMR data was used to plot a heatmap on a green-red scale (Fig. 4B). Green colour indicates a relatively lower, while red colour indicates a relatively higher level of metabolite among all the metabolic compounds within each group. In respect of the contents of released amino acids, Ile, Leu, Val, Lys, Ala, Arg, GABA and Glu demonstrated higher release levels in all groups of PFCs, whereas Trp and His exhibited the lowest relative concentration. The results agreed with previous studies that have analysed the essential amino acid profiles in pea and *N. oceanica*, both of which contained low levels of Trp and His (Du Preez, Majzoub, Thomas, Panchal, & Brown, 2021; Lu, He, Zhang, & Bing, 2020). Additionally, linoleic

acid with relatively higher release compared to other fatty acids was observed in all PFC samples, which was reasonable considering linoleic acid is the major component of sunflower oil used for making PFC in this research (Kaur, Chugh, & Gupta, 2014). For the category of sugars, the 5 sugars detected in the PFCs' digesta were generally scored low on their release content, which was as expected because the digestible polysaccharide (e.g., starch) amount in PPI and *N. oceanica* biomass should be very low according to our previous study and some other published references (Du Preez et al., 2021; Zhao et al., 2023). On the other hand, SFC showed somewhat disparity in release profile of certain metabolic compounds in comparison with PFCs, such as Gly, oleic acid, palmitic acid, β-D-Glucose and sucrose, which can be attributed to the distinct primary constituents of SFC (fish surimi and starch) and PFC (pea protein and microalgae).

3.4 Principal components analysis

To obtain a broad understanding of the metabolic variances among various groups, the separation of variables technique was employed in conducting PCA on high-throughput profiles of metabolites (Wu, Zhao, Lai, & Yang, 2021). As shown in Fig. 5A, the first two principal components (PCs) accounted for 90.6% of the total variance in the five fishcake groups, with PC1 alone explaining 81.7%. Moreover, the Q^2 value was 0.87 which exceeded 0.5, suggesting that the model was highly interpretable and had a good predictability (Wiklund, 2008). Based on the score plot depicted in Fig. 5B, the digestive samples obtained from various fishcake groups were segregated into five distinct clusters, situated at different positions along two PCs. The SFC group was located in the positive side of PC1, whereas all PFC groups were skewed towards the negative side of PC1. With the increasing proportion of *N. oceanica* in the PFCs, more significant deviations

518 from the control PFC were shown in the metabolite profiles of *N. oceanica*-incorporated PFCs,
519 leaning towards the negative side of PC2 gradually.

520 Moreover, the Euclidean distances of pairwise groups calculated according to the given
521 score variables are shown in Fig. 5C, ranging from 4.47 to 56.43 among the five groups. As
522 expected, SFC group (I) had extremely long Euclidean distances to other four groups of PFCs
523 (52.71−56.43), indicating large metabolic differences between real seafood and plant-based
524 seafood analogues. Whereas among the four PFC groups, the control group (II) and PP + NO (7:3)
525 group (V) showed the greatest inter-group distance (19.06), suggesting that the more content of *N.*
526 *oceanica* was added, the more distinct digestive performance would appear in PFCs. While the
527 score plot revealed how different groups were clustered, the loading plot revealed the metabolites
528 that were responsible for the observed separations, as illustrated in Fig. 5D. Only a few metabolites
529 such as sucrose, Gly, Ala, α-D-glucose, β-D-glucose and β-D-fructose showed large loadings on
530 PC1, while PC2 was characterised by most of the metabolites such as Leu, Arg, Ser and Glu,
531 according to each metabolite's loading plot variables shown in Table S5. These metabolites could
532 potentially serve as indicative markers that exhibited a digestive response to the addition of *N.*
533 *oceanica* in the plant-based fishcake recipe. To gain deeper insights into the impact of *N. oceanica*
534 on the digestive profile changes of PFCs, OPLS-DA, a more supervised model, was carried out
535 specifically within the pairwise PFC groups in the following section.

536

537 *3.5 Comparison of amino acid and fatty acid release within PFC pairwise groups*

538 Given the challenge of maintaining consistent sugar levels in our PFCs after incorporating
539 a mixture of pea protein and *N. oceanica* biomass at varying ratios, in this part, we decided to
540 narrow our focus on examining changes in amino acid and fatty acid release specifically. This

decision was based on the fact that the overall protein levels in all of our PFC groups remained similar (~9.3%, data not shown) and almost all the fat content was derived from the added oil, which was also consistent across PFC groups. This standardised comparison allowed us to better understand potential alterations in digestive performance resulting from the addition of the *N. oceanica* to our PFCs.

As shown in Fig. 6, three pairwise PFC groups, i.e., II and III (PP + NO (10:0) and PP + NO (9:1)), II and V (PP + NO (10:0) and PP + NO (7:3)), III and V (PP + NO (9:1) and PP + NO (7:3)), were compared respectively using established OPLS-DA models, which demonstrated good predictive and explanatory ability in all pairwise comparisons, with all R^2X values exceeding 0.977 and all Q^2 values surpassing 0.764 (data not shown). The distinct intergroup separations shown in the score plots indicated that the incorporation of *N. oceanica* into the pea protein-based fishcake analogue could cause a discernible impact on the release of metabolites after *in vitro* digestion, aligning with the separated metabolomes observed on the PCA score plots. Furthermore, statistical analysis was performed using coefficient plots to identify significant metabolites that contributed to the inter-group differentiation, which varied with the change of *N. oceanica* addition concentration (right side of Fig. 6A-C). A positive coefficient indicated a *N. oceanica*-induced increase, while a negative coefficient indicated a *N. oceanica*-induced decrease in content of the amino acid and fatty acid release of PFCs. The variables with VIP values greater than 1 were considered as significantly discriminative metabolites contributing to the group separation, which were marked in red specifically (Zhao et al., 2022).

In terms of amino acid release, the addition of *N. oceanica* at lower concentration (10%) already elicited a significant decrease in the levels of Ile, Gln, Arg, Leu and GABA in the PFC digesta (Fig. 6A), and when the concentration of *N. oceanica* continued to increase, the release

564 levels of Leu, Arg and GABA exhibited further declining trends, whereas the release trends of Ala,
565 Gly, Ile and Gln went in the opposite direction (Fig. 6C). Interestingly, the contents of most
566 hydrophobic amino acids, such as Val, Met, Gly, Phe and Leu, as well as a range of hydrophilic
567 amino acids, including Asp, Tyr, Asn, Thr, Ser, Arg and Glu, showed pronounced decreased trends
568 in the digesta of PFC with a higher concentration of *N. oceanica* (30%) (Fig. 6B), indicating the
569 amino acid bioavailability of PP + NO (7:3) group was altered markedly as compared to that in
570 the control PFC group.

571 According to the findings in Section 3.2 and Section 3.5, the amount of amino acid released
572 after *in vitro* digestion was not always proportional to the level of protein digested. Previous works
573 have shown that pea proteins are primarily found as globulins (55−65%), while phycobiliproteins
574 (PBPs) with highly preserved structural characteristics make up the primary constituents (85%) of
575 phycobilisomes (PBSs) in microalgae (Asen & Aluko, 2022; Dagnino-Leone et al., 2022). The
576 functional structures of PBSs, namely the rods and the core, are formed by hexamers $(\alpha\beta)_6$ and
577 trimers $(\alpha\beta)_3$ of PBPs consisting of α and β subunits, which were found capable of returning to
578 their native state when the denaturing conditions such as high temperature and chemical
579 disturbances were removed (MacColl, Eisele, & Menikh, 2003). On the other hand, it has been
580 observed that the tertiary and quaternary structures of pea proteins could undergo irreversible
581 changes under processing conditions, followed by higher degree of hydrolysis (Ma, Boye, & Hu,
582 2017). Therefore, our findings indicated that the proteins in *N. oceanica* might be more tightly
583 packed and less sensitive compared to the globular structure of pea proteins after PFC processing,
584 resulting in fewer sites available for enzymatic actions and leading to a reduced release of most
585 amino acids in the PP + NO (7:3) group.

586 Besides the protein type and structural organization, the composition and sequence of
587 amino acids are also important factors that affect the digestion process and the bioavailability of
588 amino acids (Xie et al., 2022). It is known that during the gastric digestion stage, pepsin typically
589 cleaves after hydrophobic amino acids like Leu and Phe, followed by two other aromatic amino
590 acids, Trp and Tyr (Ahn, Cao, Yu, & Engen, 2013). Whereas during intestinal digestion, trypsin
591 favors peptide bonds where basic amino acids Lys and Arg contribute the carboxyl group (Ahmed,
592 Sun, & Udenigwe, 2022). Therefore, the decreased levels of Leu, Phe, Tyr and Arg observed in
593 the *N. oceanica*-incorporated PFCs suggested that the amounts of these amino acids in *N. oceanica*
594 proteins might be lower than those in the pea proteins used in our PFCs, which were consistent
595 with previous reports (Banaszek et al., 2019; Du Preez et al., 2021). Furthermore, the arrangement
596 of these amino acids in *N. oceanica* proteins might not be well-suited to bind to digestive enzymes'
597 active sites, compromising the efficiency of these enzymes in cleaving proteins into smaller
598 peptides or free amino acids during digestion.
599 In addition to the release of amino acids, the fatty acid profiles following *in vitro* digestion
600 is also a crucial indicator of the nutritional value of our PFC. According to the coefficient plot in
601 Fig. 6A, introducing *N. oceanica* at a lower concentration (10%) led to a significant decrease in
602 the release of oleic acid, palmitic acid, and linoleic acid in the PFC digesta. As the concentration
603 of *N. oceanica* increased, the release of linoleic acid continued to decrease while the release of
604 oleic acid and palmitic acid started to increase, a phenomenon demonstrated in both Fig. 6B and
605 6C. Given the negligible fat content in both of the PPI and defatted *N. oceanica* biomass (as
606 indicated in Table S1 at 0.2% and 0.1% respectively), we incorporated sunflower oil in the current
607 study to improve the palatability, texture, and taste of our PFC (Ahmad et al., 2022). Earlier
608 research has indicated that the unsaturated fatty acid (USFA) content of sunflower oil comprises

609 approximately 85% (with 14–43% oleic acid and 44–75% linoleic acid in the USFA composition),
610 while the remaining 15% is saturated fatty acids (SFA, palmitic acid is one of the most common
611 therein) (Akkaya, 2018). All the fatty acids detected after digestion matched the fatty acid profiles
612 of sunflower oil in present study, since almost all of them were derived from it.

613 It has been proposed that the extent of lipolysis during food digestion could be significantly
614 influenced by the way lipids interact with other non-lipid components within the food matrix, such
615 as lipid–protein, SFA–protein and lipid–starch interactions (Calvo-Lerma, Fornés-Ferrer, Heredia,
616 & Andrés, 2018). As linoleic acid is the most abundant fatty acid in our PFCs, its significantly
617 reduced release in all *N. oceanica*-incorporated PFCs might be also linked to the *N. oceanica*
618 proteins' ability to form a higher gel structure as stated earlier, which could trap more lipids within
619 their structures and limit the diffusion capacity of lipase to the fat droplet interface during digestion
620 (Grundy et al., 2016). Furthermore, as mentioned above, the incorporation of *N. oceanica* in the
621 PFC groups might result in a higher viscosity of the digestion medium, which could also hinder
622 the lipase's ability to access the fat, resulting in a noticeable reduction in the dominant fatty acid
623 (i.e., linoleic acid). However, on the other hand, some studies have demonstrated that bile salts as
624 bio-surfactants can remove proteins that may exist at the interface, increasing the ability of lipase
625 to effectively operate on the hydrophobic lipid core and thereby enhancing lipolysis (Maldonado-
626 Valderrama, Wilde, Macierzanka, & Mackie, 2011; Sarkar, Ye, & Singh, 2016). Thus, the reduction
627 in the availability of lipase to break down fat caused by the lipid–protein interactions might be
628 somewhat counteracted by the ability of bile salts to remove proteins at the oil–water boundary.
629 This could explain why a rise in the concentrations of certain fatty acids with a relatively small
630 amount, such as oleic acid and palmitic acid, was observed in the digesta of PFC containing a
631 higher proportion (30%) of *N. oceanica*.

3.6 Alterations of amino acid and fatty acid metabolisms of PFC during digestion

In order to thoroughly investigate the changes in metabolic networks caused by the presence of *N. oceanica* in PFC during digestion, we conducted an enrichment analysis on the amino acid and fatty acid metabolisms, focusing on those metabolites that were significantly affected (with VIP > 1) in the PP + NO (7:3) group as shown in Section 3.5. Fig. 7A provides a summary of the top 25 metabolic pathways that were enriched, and those with a significance level of $P < 0.05$ and enrichment ratio > 15 were identified as the most impacted by the addition of *N. oceanica* (Ran, Yang, et al., 2022). Eight particularly affected pathways were found to meet these criteria, namely aminoacyl-tRNA biosynthesis, valine, leucine and isoleucine biosynthesis, alanine, aspartate and glutamate metabolism, arginine biosynthesis, phenylalanine, tyrosine and tryptophan biosynthesis, D-glutamine and D-glutamate metabolism, nitrogen metabolism and phenylalanine metabolism. Furthermore, a proposed metabolic map was illustrated in Fig. 7B based on KEGG and related databases, with metabolites highlighted in red or green indicating higher or lower content, respectively, in the PP + NO (7:3) group as compared to those in the control PFC group.

The human body relies on amino acid metabolism to facilitate various biological reactions, which are crucial for maintaining health and promoting growth (Wu, 2009). One significant example is the role of branched-chain amino acids (BCAA) in modulating metabolic health in response to dietary protein intake. Studies have linked increased levels of the three BCAAs (Leu, Ile, and Val) in humans to the development of insulin resistance and diabetes (Arany & Neinast, 2018; Würtz et al., 2013). Additionally, higher concentrations of two aromatic amino acids (Phe and Tyr) in the bloodstream have been associated with reduced insulin sensitivity as well (Würtz et al., 2013). Therefore, the decreased amounts of Leu, Val, Phe and Tyr detected in the PP + NO

(7:3) group suggested that the addition of *N. oceanica* to PFC could potentially intervene in Val, Leu and Ile biosynthesis and Phe, Tyr, and Trp biosynthesis during digestion, playing an important role in modifying the amino acid composition of diets for individuals with diabetic complications. On the other hand, Gln is known for its significant contribution to cell metabolism, such as aiding in the tricarboxylic acid cycle and biosynthesis of nucleotides (Yoo, Yu, Sung, & Han, 2020). Thus, our *N. oceanica*-incorporated PFC could provide a source of Gln for individuals with compromised immune systems by releasing higher levels of this amino acid during digestion, serving as a valuable addition to nutrition supplementation. Moreover, it has been demonstrated previously that limiting the intake of sulphur-containing amino acids, especially Met and Cys, can provide health benefits against age-related diseases (Richie Jr et al., 2023). Therefore, the utilisation of *N. oceanica* in PFC as studied here could potentially delay the aging process in human body by reducing the release of Met during digestion.

In addition to its impact on amino acid metabolism, the introduction of *N. oceanica* might also affect the fatty acid metabolism of PFC during digestion. The levels of palmitic acid (C16:0) and oleic acid (C18:1 ω-9) were found to increase, while the level of linoleic acid (C18:2 ω-6) decreased in the digesta of PFC with a higher concentration of *N. oceanica* (30%) (Fig. 7B). These changes might cause a shift in the activity of acetyl-CoA in the human body, which in turn could also lead to alterations in the biosynthesis of saturated and unsaturated fatty acids successively as acetyl-CoA serves as a precursor for fatty acid biosynthesis (Oliver, Nikolau, & Wurtele, 2009). Prior research has indicated that while an appropriate amount of palmitic acid can aid in maintaining metabolic health, excessive intake of it can ultimately result in heart failure (Harun, 2019). Thus, from a human health standpoint, it is preferable to limit palmitic acid intake. On the other hand, unsaturated fatty acids are generally considered beneficial. Oleic acid is known to have

678 positive effects on various tissues with rare negative impacts, while a high level of linoleic acid in
679 the bloodstream has been linked to a lower blood cholesterol level and reduced risk of
680 atherosclerosis and cardiovascular disease (Harun, 2019; Sales-Campos, Reis de Souza, Crema
681 Peghini, Santana da Silva, & Ribeiro Cardoso, 2013). Therefore, our findings can provide
682 consumers, especially those at a higher risk of cardiovascular disease, with more information about
683 our *N. oceanica*-incorporated PFC from the point of metabolism to aid in their future purchase
684 decision-making.
685
686 *3.7 Comparison of microstructure before and after* in vitro *digestion*
687 The SEM analysis at 300× magnification captured the microstructures of SFC and PFCs
688 before and after *in vitro* digestion, as presented in Fig. 8. Prior to digestion, the SFC exhibited a
689 compact and uniform gel structure with regularly distributed honeycomb-like pores within its
690 fibrous and continuous networks (Fig. 8A). For PFC samples, the control PFC showed a
691 fragmented and discontinuous microstructure with noticeable wide gaps (Fig. 8B, highlighted by
692 red arrows), indicating a loose and soft texture consistent with the findings in Section 3.1.1. In
693 contrast, the addition of *N. oceanica* to PFCs resulted in a more cohesive surface morphology. As
694 the concentration of *N. oceanica* increased, the size of the pores and interspaces decreased, and
695 their distribution became more regular, resulting in denser and firmer PFC gels. The small and
696 unevenly distributed spots, indicated by red arrows (Fig. 8E), could be attributed to the presence
697 of *N. oceanica* biomass, contributing to a rougher surface of the PFCs.
698 Following *in vitro* digestion, the SFC digesta exhibited a higher degree of dissociation and
699 fragmentation, with broken and wrinkled surfaces (Fig. 8a). In comparison, the digesta of PFCs
700 maintained respective structures to a large extent after undergoing digestive enzymatic actions,

with fewer incomplete and broken fragments (Fig. 8b−e). Notably, PFC with higher *N. oceanica* content displayed a coarser appearance, characterised by the presence of additional spots on the surface of the digesta (indicated by red arrows in Fig. 8e). This observation could be attributed to the enzymatic effects on the microalgae during digestion. As mentioned in Section 3.2, the increased viscosity of the digesta caused by *N. oceanica* and the release of indigestible fibres from *N. oceanica* biomass could impede the action of digestive enzymes, thereby delaying the digestion process of PFCs. Consequently, the digesta structure of *N. oceanica*-incorporated PFCs appeared more complete and continuous compared to that of SFC. Therefore, the SEM images corroborated the textural and digestibility results discussed earlier.

4. Conclusion

As the concentration of *N. oceanica* increased, the observed changes in the physical properties of *N. oceanica*-incorporated PFC became more pronounced. These changes included increased hardness, decreased springiness, reduced expressible moisture and oil contents, and stronger gel strength. The incorporation of defatted *N. oceanica* could induce the formation of well-structured gel matrices, leading to denser gel networks and enhanced textural properties that more closely resembled those of the SFC counterpart. For digestive performance, lower *N. oceanica* concentration (10%) in PFC increased the *in vitro* protein digestibility, but the effect was reduced with higher *N. oceanica* concentration (30%), which might be due to the limited enzyme-protein interactions caused by elevated viscosity in the PFC digesta and more indigestible components (e.g., fibres) from *N. oceanica* biomass introduced to the PFC gel system. The NMR-based foodomic profiling showed that the presence of *N. oceanica* in PFCs led to a suppression in the release of certain amino acids (such as hydrophobic amino acids) and fatty acids (such as

linoleic acid) during *in vitro* digestion, which could potentially impact a series of amino acid biosynthesis and fatty acid metabolisms in the human body following consumption. The SEM micrographs provided supporting evidence that the incorporation of *N. oceanica* in PFC resulted in a more compact structure, which remained relatively intact even after digestion. Overall, this study addressed the existing research gaps by investigating the impact of *Nannochloropsis* on the physical properties and digestive profiles of plant-based fishcake. Despite *Nannochloropsis* sp. not having received novel food authorization yet due to the challenges in meeting all the stringent safety requirements set by current law, there is anticipated growth in patents and permissions for food products linked to *Nannochloropsis* sp. That's why it's important to assess the physical properties and digestive performance of these *Nannochloropsis*-enriched food products before putting them on the market. In future studies, we aim to explore the intricate interactions between macromolecules (such as microalgae, gums, and PPI) within our PFC gel system and thoroughly assess its sensory qualities.

CRediT authorship contribution statement

Lin Zhao: Conceptualization, Methodology, Investigation, Software, Visualization, Writing-original draft, Writing-review & editing. **Hui Mei Khang:** Methodology, Investigation, Visualization, Writing-original draft. **Juan Du:** Funding acquisition, Conceptualization, Methodology, Project administration, Supervision, Writing-review & editing.

Declaration of competing interest

None.

Acknowledgements

This study was funded by Singapore Food Story Theme 2–1st Alternative Protein Seed Challenge Grant (W20W2D0019 and W20W2D0013), and Singapore Food Story R&D Programme Industry Alignment Fund Pre-positioning (IAF-PP) Theme 2–Advanced Biotech-based Protein Production Grant (A21H7a0131 and H21H8a0005), administered by A*STAR. We would like to thank Dr. Michael Voigtmann, Dr. Sergei Belyakov from Wintershine Asia Pte Ltd, Dr. Maria N. Antipina from SIFBI A*STAR for their support and assistance. We would also like to thank the previous and present lab mates, Ms. Felicia Peh Zhi Wen, Mr. Cedric Sow Wee Jian, and Mr. Jeremy Chin Tak Gun, for their kindness and assistance.

References

Abdol Rahim Yassin, Z., Binte Abdul Halim, F. N., Taheri, A., Goh, K. K. T., & Du, J. (2023). Effects of microwave, ultrasound, and high-pressure homogenization on the physicochemical properties of sugarcane fibre and its application in white bread. *LWT, 184,* 115008.

Ahmad, M., Qureshi, S., Akbar, M. H., Siddiqui, S. A., Gani, A., Mushtaq, M., Hassan, I., & Dhull, S. B. (2022). Plant-based meat alternatives: Compositional analysis, current development and challenges. *Applied Food Research, 2*(2), 100154.

Ahmed, T., Sun, X., & Udenigwe, C. C. (2022). Role of structural properties of bioactive peptides in their stability during simulated gastrointestinal digestion: A systematic review. *Trends in Food Science & Technology, 120,* 265-273.

Ahn, J., Cao, M.-J., Yu, Y. Q., & Engen, J. R. (2013). Accessing the reproducibility and specificity of pepsin and other aspartic proteases. *Biochimica et Biophysica Acta (BBA)-Proteins and Proteomics, 1834*(6), 1222-1229.

Akkaya, M. R. (2018). Prediction of fatty acid composition of sunflower seeds by near-infrared reflectance spectroscopy. *Journal of Food Science and Technology, 55*, 2318-2325.

Allied Market Research. (2022). *Plant-based seafood market report. Plant-based seafood market by product (fish products, prawn and shrimp products, crab products), by source (soy, wheat, pea, canola, lentil, others), by distribution channel (supermarkets and hypermarkets, specialty stores, horeca, convenience stores, online sales), by consumer (omnivore, flexitarian, vegetarian, vegan): global opportunity analysis and industry forecast, 2021-2031*. Retrieved from https://www.alliedmarketresearch.com/plant-based-seafood-market-A17387. Accessed May 31, 2023.

Annamalai, S. N., Das, P., Thaher, M. I., Abdul Quadir, M., Khan, S., Mahata, C., & Al Jabri, H. (2021). Nutrients and energy digestibility of microalgal biomass for fish feed applications. *Sustainability, 13*(23), 13211.

AOAC. (2005). *Official methods of analysis* (18th ed.). Pub AOAC International Maryland.

Arany, Z., & Neinast, M. (2018). Branched chain amino acids in metabolic disease. *Current Diabetes Reports, 18*, 1-8.

Asen, N. D., & Aluko, R. E. (2022). Physicochemical and functional properties of membrane-fractionated heat-induced pea protein aggregates. *Frontiers in Nutrition, 9*, 852225.

Atitallah, A. B., Barkallah, M., Hentati, F., Dammak, M., Hlima, H. B., Fendri, I., Attia, H., Michaud, P., & Abdelkafi, S. (2019). Physicochemical, textural, antioxidant and sensory

790 characteristics of microalgae-fortified canned fish burgers prepared from minced flesh of
791 common barbel (*Barbus barbus*). *Food Bioscience, 30*, 100417.
792 Banaszek, A., Townsend, J. R., Bender, D., Vantrease, W. C., Marshall, A. C., & Johnson, K. D.
793 (2019). The effects of whey vs. pea protein on physical adaptations following 8-weeks of
794 high-intensity functional training (HIFT): A pilot study. *Sports, 7*(1), 12.
795 Becker, E. W. (2007). Micro-algae as a source of protein. *Biotechnology Advances, 25*(2), 207-
796 210.
797 Binte Abdul Halim, F. N., Taheri, A., Abdol Rahim Yassin, Z., Chia, K. F., Goh, K. K. T., Goh,
798 S. M., & Du, J. (2023). Effects of Incorporating Alkaline Hydrogen Peroxide Treated
799 Sugarcane Fibre on The Physical Properties and Glycemic Potency of White Bread. Foods,
800 12(7), 1460.
801 Bornhorst, G. M., Ferrua, M. J., & Singh, R. P. (2015). A proposed food breakdown classification
802 system to predict food behavior during gastric digestion. *Journal of Food Science, 80*(5),
803 R924-R934.
804 Bourne, M. (2002). *Food texture and viscosity: concept and measurement*: Elsevier.
805 Calvo- Lerma, J., Fornés- Ferrer, V., Heredia, A., & Andrés, A. (2018). *In vitro* digestion of lipids
806 in real foods: influence of lipid organization within the food matrix and interactions with
807 nonlipid components. *Journal of Food Science, 83*(10), 2629-2637.
808 Caporgno, M. P., Böcker, L., Müssner, C., Stirnemann, E., Haberkorn, I., Adelmann, H.,
809 Handschin, S., Windhab, E. J., & Mathys, A. (2020). Extruded meat analogues based on
810 yellow, heterotrophically cultivated *Auxenochlorella protothecoides* microalgae.
811 *Innovative Food Science & Emerging Technologies, 59*, 102275.

812 Caporgno, M. P., & Mathys, A. (2018). Trends in microalgae incorporation into innovative food
813 products with potential health benefits. *Frontiers in Nutrition, 5*, 58.
814 Chaijan, M., Panpipat, W., & Benjakul, S. (2010). Physicochemical and gelling properties of short-
815 bodied mackerel (*Rastrelliger brachysoma*) protein isolate prepared using alkaline-aided
816 process. *Food and Bioproducts Processing*, *88*(2-3), 174-180.
817 Chen, C., Tang, T., Shi, Q., Zhou, Z., & Fan, J. (2022). The potential and challenge of microalgae
818 as promising future food sources. *Trends in Food Science & Technology, 126*, 99-112.
819 Coleman, B., Van Poucke, C., Dewitte, B., Ruttens, A., Moerdijk-Poortvliet, T., Latsos, C., Reu,
820 K. D., Blommaert, L., Duquenne, B., Timmermans, K., Houcke, J. v., Muylaert, K., &
821 Robbens, J. (2022). Potential of microalgae as flavoring agents for plant-based seafood
822 alternatives. *Future Foods, 5*, 100139.
823 Dagnino-Leone, J., Figueroa, C. P., Castañeda, M. L., Youlton, A. D., Vallejos-Almirall, A.,
824 Agurto-Muñoz, A., Pérez, J. P., & Agurto-Muñoz, C. (2022). Phycobiliproteins: Structural
825 aspects, functional characteristics, and biotechnological perspectives. *Computational and*
826 *Structural Biotechnology Journal, 20*, 1506-1527.
827 Du Preez, R., Majzoub, M. E., Thomas, T., Panchal, S. K., & Brown, L. (2021). *Nannochloropsis*
828 *oceanica* as a microalgal food intervention in diet-induced metabolic syndrome in rats.
829 *Nutrients, 13*(11), 3991.
830 Gerde, J. A., Wang, T., Yao, L., Jung, S., Johnson, L. A., & Lamsal, B. (2013). Optimizing protein
831 isolation from defatted and non-defatted *Nannochloropsis* microalgae biomass. *Algal*
832 *Research, 2*(2), 145-153.
833 Graça, C., Fradinho, P., Sousa, I., & Raymundo, A. (2018). Impact of *Chlorella vulgaris* on the
834 rheology of wheat flour dough and bread texture. *LWT, 89*, 466-474.

Grundy, M. M., Carrière, F., Mackie, A. R., Gray, D. A., Butterworth, P. J., & Ellis, P. R. (2016). The role of plant cell wall encapsulation and porosity in regulating lipolysis during the digestion of almond seeds. *Food & Function, 7*(1), 69-78.

Harun, M. (2019). Fatty acid composition of sunflower in 31 inbreed and 28 hybrid. *Biomedical Journal of Scientific & Technical Research, 16*(3), 12032-12038.

Hernández-López, I., Valdés, J. R. B., Castellari, M., Aguiló-Aguayo, I., Morillas-España, A., Sánchez-Zurano, A., Acién-Fernández, F. G., & Lafarga, T. (2021). Utilisation of the marine microalgae *Nannochloropsis* sp. and *Tetraselmis* sp. as innovative ingredients in the formulation of wheat tortillas. *Algal Research, 58*, 102361.

Kaur, N., Chugh, V., & Gupta, A. K. (2014). Essential fatty acids as functional components of foods-a review. *Journal of Food Science and Technology, 51*, 2289-2303.

Kazir, M., & Livney, Y. D. (2021). Plant-based seafood analogs. *Molecules*, *26*(6), 1559.

Kumar, M., Tomar, M., Punia, S., Dhakane-Lad, J., Dhumal, S., Changan, S., Senapathy, M., Berwal, M. K., Sampathrajan, V., Sayed, A. A., Chandran, D., Pandiselvam R., Rais, N., Mahato, D. K., Udikeri, S. S., Satankar, V., Anitha, T., Reetu, Radha, Singh, S., Amarowicz, R., & Kennedy, J. F. (2022). Plant-based proteins and their multifaceted industrial applications. *LWT, 154*, 112620.

Li, L., Wang, N., Ma, S., Yang, S., Chen, X., Ke, Y., & Wang, X. (2018). Relationship of moisture status and quality characteristics of fresh wet noodles prepared from different grade wheat flours from flour milling streams. *Journal of Chemistry, 2018*, 7464297.

Lu, Z., He, J., Zhang, Y., & Bing, D. (2020). Composition, physicochemical properties of pea protein and its application in functional foods. *Critical Reviews in Food Science and Nutrition, 60*(15), 2593-2605.

Ma, Z., Boye, J. I., & Hu, X. (2017). *In vitro* digestibility, protein composition and techno-functional properties of Saskatchewan grown yellow field peas (*Pisum sativum* L.) as affected by processing. *Food Research International, 92*, 64-78.

MacColl, R., Eisele, L. E., & Menikh, A. (2003). Allophycocyanin: trimers, monomers, subunits, and homodimers. *Biopolymers, 72*(5), 352-365.

Maldonado-Valderrama, J., Wilde, P., Macierzanka, A., & Mackie, A. (2011). The role of bile salts in digestion. *Advances in Colloid and Interface Science, 165*(1), 36-46.

Martins, C. F., Trevisi, P., Coelho, D. F., Correa, F., Ribeiro, D. M., Alfaia, C. M., Pinho, M., Pestana, J. M., Mourato, M. P., Almeida, A. M., Fontes, C. M. G. A., Freire, J. P. B., & Prates, J. A. M. (2022). Influence of *Chlorella vulgaris* on growth, digestibility and gut morphology and microbiota of weaned piglet. *Scientific Reports, 12*(1), 6012.

Minekus, M., Alminger, M., Alvito, P., Ballance, S., Bohn, T., Bourlieu, C., Carrière, F., Boutrou, R., Corredig, M., Dupont, D., Dufour, C., Egger, L., Golding, M., Karakaya, S., Kirkhus, B., Feunteun, S. L., Lesmes, U., Macierzanka, A., Mackie, A., Marze, S., McClements, D. J., Ménard, O., Recio, I., Santos, C. N., Singh, R. P., Vegarud, G. E., Wickham, M. S. J., Weitschies, W., & Brodkorb, A. (2014). A standardised static *in vitro* digestion method suitable for food–an international consensus. *Food & Function, 5*(6), 1113-1124.

Nasrin, T. A. A., Noomhorm, A., & Anal, A. K. (2015). Physico-chemical characterization of culled plantain pulp starch, peel starch, and flour. *International Journal of Food Properties*, *18*(1), 165-177.

Neumann, U., Derwenskus, F., Gille, A., Louis, S., Schmid-Staiger, U., Briviba, K., & Bischoff, S. C. (2018). Bioavailability and safety of nutrients from the microalgae *Chlorella vulgaris*,

Nannochloropsis oceanica and *Phaeodactylum tricornutum* in C57BL/6 mice. *Nutrients*, *10*(8), 965.

Oliver, D. J., Nikolau, B. J., & Wurtele, E. S. (2009). Acetyl-CoA—life at the metabolic nexus. *Plant Science, 176*(5), 597-601.

Palanisamy, M., Töpfl, S., Berger, R. G., & Hertel, C. (2019). Physico-chemical and nutritional properties of meat analogues based on *Spirulina*/lupin protein mixtures. *European Food Research and Technology, 245*, 1889-1898.

Paterson, S., Gómez-Cortés, P., de la Fuente, M. A., & Hernández-Ledesma, B. (2023). Bioactivity and digestibility of microalgae *Tetraselmis* sp. and *Nannochloropsis* sp. as basis of their potential as novel functional foods. *Nutrients*, *15*(2), 477.

Ran, X., Lou, X., Zheng, H., Gu, Q., & Yang, H. (2022). Improving the texture and rheological qualities of a plant-based fishball analogue by using konjac glucomannan to enhance crosslinks with soy protein. *Innovative Food Science & Emerging Technologies, 75*, 102910.

Ran, X., Yang, Z., Chen, Y., & Yang, H. (2022). Konjac glucomannan decreases metabolite release of a plant-based fishball analogue during *in vitro* digestion by affecting amino acid and carbohydrate metabolic pathways. *Food Hydrocolloids*, *129*, 107623.

Richie Jr, J. P., Sinha, R., Dong, Z., Nichenametla, S. N., Ables, G. P., Ciccarella, A., Sinha, I., Calcagnotto, A. M., Chinchilli, V. M., Reinhart, L., & Orentreich, D. (2023). Dietary methionine and total sulfur amino acid restriction in healthy adults. *The Journal of Nutrition, Health & Aging*, *27*(2), 111-123.

Sales-Campos, H., Reis de Souza, P., Crema Peghini, B., Santana da Silva, J., & Ribeiro Cardoso, C. (2013). An overview of the modulatory effects of oleic acid in health and disease. *Mini Reviews in Medicinal Chemistry, 13*(2), 201-210.

Samtiya, M., Aluko, R. E., & Dhewa, T. (2020). Plant food anti-nutritional factors and their reduction strategies: an overview. *Food Production, Processing and Nutrition, 2*, 1-14.

Sarkar, A., Ye, A., & Singh, H. (2016). On the role of bile salts in the digestion of emulsified lipids. *Food Hydrocolloids, 60*, 77-84.

Shamasundar, B. (2023). Surimi and suimi-based products. In *Advances in fish processing technologies* (pp. 31-52). Apple Academic Press.

Taheri, A., Kashaninejad, M., Tamaddon, A. M., Du, J., & Jafari, S. M. (2023). Rheological Characteristics of Soluble Cress Seed Mucilage and β-Lactoglobulin Complexes with Salts Addition: Rheological Evidence of Structural Rearrangement. *Gels, 9*(6), 485.

Vidal, N. P., Picone, G., Goicoechea, E., Laghi, L., Manzanos, M. J., Danesi, F., Bordoni, A., Capozzi, F., & Guillén, M. D. (2016). Metabolite release and protein hydrolysis during the *in vitro* digestion of cooked sea bass fillets. A study by ^{1}H NMR. *Food Research International, 88*, 293-301.

Wang, M., Yin, Z., Sun, W., Zhong, Q., Zhang, Y., & Zeng, M. (2023). Microalgae play a structuring role in food: Effect of *spirulina platensis* on the rheological, gelling characteristics, and mechanical properties of soy protein isolate hydrogel. *Food Hydrocolloids, 136*, 108244.

Wang, Y., Kim, W., Naik, R. R., Spicer, P. T., & Selomulya, C. (2023). Tuning the pea protein gel network to mimic the heterogenous microstructure of animal protein. *Food Hydrocolloids, 140*, 108611.

Wang, Y., Tibbetts, S. M., & McGinn, P. J. (2021). Microalgae as sources of high-quality protein for human food and protein supplements. *Foods, 10*(12), 3002.

Wiklund, S. (2008). *Multivariate data analysis for Omics*. Umea: Umetrics.

Wu, G. (2009). Amino acids: metabolism, functions, and nutrition. *Amino Acids, 37*, 1-17.

Wu, J., Zhao, L., Lai, S., & Yang, H. (2021). NMR-based metabolomic investigation of antimicrobial mechanism of electrolysed water combined with moderate heat treatment against *Listeria monocytogenes* on salmon. *Food Control, 125*, 107974.

Würtz, P., Soininen, P., Kangas, A. J., Rönnemaa, T., Lehtimäki, T., Kähönen, M., Viikari, J. S., Raitakari, O. T., & Ala-Korpela, M. (2013). Branched-chain and aromatic amino acids are predictors of insulin resistance in young adults. *Diabetes Care, 36*(3), 648-655.

Xie, Y., Cai, L., Zhao, D., Liu, H., Xu, X., Zhou, G., & Li, C. (2022). Real meat and plant-based meat analogues have different *in vitro* protein digestibility properties. *Food Chemistry, 387*, 132917.

Yan, B., Jiao, X., Zhu, H., Wang, Q., Huang, J., Zhao, J., Cao, H., Zhou, W., Zhang, W., Ye, W., Zhang, H., & Fan, D. (2020). Chemical interactions involved in microwave heat-induced surimi gel fortified with fish oil and its formation mechanism. *Food Hydrocolloids, 105*, 105779.

Yang, F., Cheng, C., Long, L., Hu, Q., Jia, Q., Wu, H., & Xiang, W. (2015). Extracting lipids from several species of wet microalgae using ethanol at room temperature. *Energy & Fuels, 29*(4), 2380-2386.

Yoo, H. C., Yu, Y. C., Sung, Y., & Han, J. M. (2020). Glutamine reliance in cell metabolism. *Experimental & Molecular Medicine, 52*(9), 1496-1516.

Zanella, L., & Vianello, F. (2020). Microalgae of the genus *Nannochloropsis*: Chemical composition and functional implications for human nutrition. *Journal of Functional Foods, 68*, 103919.

Zhao, L., Chen, M.-H., Bi, X., & Du, J. (2023). Physicochemical properties, structural characteristics and *in vitro* digestion of brown rice–pea protein isolate blend treated by microbial transglutaminase. *Food Hydrocolloids, 141*, 108673.

Zhao, L., Poh, C. N., Wu, J., Zhao, X., He, Y., & Yang, H. (2022). Effects of electrolysed water combined with ultrasound on inactivation kinetics and metabolite profiles of *Escherichia coli* biofilms on food contact surface. *Innovative Food Science & Emerging Technologies, 76*, 102917.

Zhao, L., Zhao, X., Wu, J. e., Lou, X., & Yang, H. (2019). Comparison of metabolic response between the planktonic and air-dried *Escherichia coli* to electrolysed water combined with ultrasound by ^{1}H NMR spectroscopy. *Food Research International, 125*, 108607.

Figure captions:

Fig. 1. The hardness (A), springiness (B), expressible moisture (C) and expressible oil (D) of surimi-based fishcake and plant-based fishcake analogues at different *Nannochloropsis oceanica* addition. Note: PP + NO (10:0), (9:1), (8:2) and (7:3) represent the ratio of pea protein isolate and *Nannochloropsis oceanica* in plant-based fishcake analogues, respectively. The detailed ingredients used in each group are shown in Table S2. Significant differences are indicated by groups with distinct letters.

Fig. 2. Effects of *Nannochloropsis oceanica* concentration on shear strain dependence (A) and frequency dependence (B) of storage modulus (G') for plant-based fishcake analogues. Note: PP + NO (10:0), (9:1), (8:2) and (7:3) represent the ratio of pea protein isolate and *Nannochloropsis oceanica* in plant-based fishcake analogues, respectively. The detailed ingredients used in each group are shown in Table S2. The G' value of surimi-based fishcake is served as a reference. Data are presented as mean values.

Fig. 3. Protein digestibility of surimi-based fishcake and plant-based fishcake analogues after *in vitro* digestion. Note: PP + NO (10:0), (9:1), (8:2) and (7:3) represent the ratio of pea protein isolate and *Nannochloropsis oceanica* in plant-based fishcake analogues, respectively. The detailed ingredients used in each group are shown in Table S2. Significant differences are indicated by groups with distinct letters.

Fig. 4. Representative ^{1}H NMR spectra (A) and heatmap (B) of the metabolites in the digesta of surimi-based fishcake (SFC) and plant-based fishcake (PFC) analogues at different *Nannochloropsis oceanica* addition after *in vitro* digestion. Note: the groups labelled I-V correspond to SFC, PP + NO (10:0), PP + NO (9:1), PP + NO (8:2), and PP + NO (7:3), respectively. The detailed ingredients used in each PFC group are shown in Table S2. The representative numbers of metabolites are the same as those in Table S4.

Fig. 5. Principal component analysis (PCA) for the metabolite profile of surimi-based fishcake (SFC) and plant-based fishcake (PFC) analogues at different *Nannochloropsis oceanica* addition after *in vitro* digestion. The principal components explaining variances used in PCA (A); PCA

score plot (B); Euclidean distances among the variables (C); PCA loading plot (D). Note: the groups labelled I-V correspond to SFC, PP + NO (10:0), PP + NO (9:1), PP + NO (8:2), and PP + NO (7:3), respectively. The detailed ingredients used in each PFC group are shown in Table S2.

Fig. 6. Orthogonal partial least squares discriminant analysis (OPLS-DA) of pairwise PFC groups. The OPLS-DA score plot and OPLS coefficient plot of groups II-III (A), groups II-V (B) and groups III-V (C). Note: group II, III, and V correspond to PP + NO (10:0), PP + NO (9:1), and PP + NO (7:3), respectively. The detailed ingredients used in each group are shown in Table S2. Metabolites coloured in red contributed significantly to the OPLS-DA models (VIP > 1).

Fig. 7. Overview of the enrichment analysis (A) and proposed schematic of metabolic alterations in the digesta of plant-based fishcake (PFC) analogue in the PP + NO (7:3) group (B). Note: Metabolites coloured in green, red or black represent lower, higher or similar level in the PP + NO (7:3) group as compared to those in the control PFC group, respectively; metabolites with italic font indicate those that were not identified in this study. The detailed ingredients used in the control PFC (PP + NO (10:0)) group and the PP + NO (7:3) group are shown in Table S2.

Fig. 8. The surface microstructure of surimi-based fishcake (SFC) and plant-based fishcake (PFC) analogues before *in vitro* digestion (A−E) and after *in vitro* digestion (a−e). Note: (A) and (a): SFC; (B) and (b): PP + NO (10:0); (C) and (c): PP + NO (9:1); (D) and (d): PP + NO (8:2); (E) and (e): PP + NO (7:3). The detailed ingredients used in each PFC group are shown in Table S2.

Figure 1

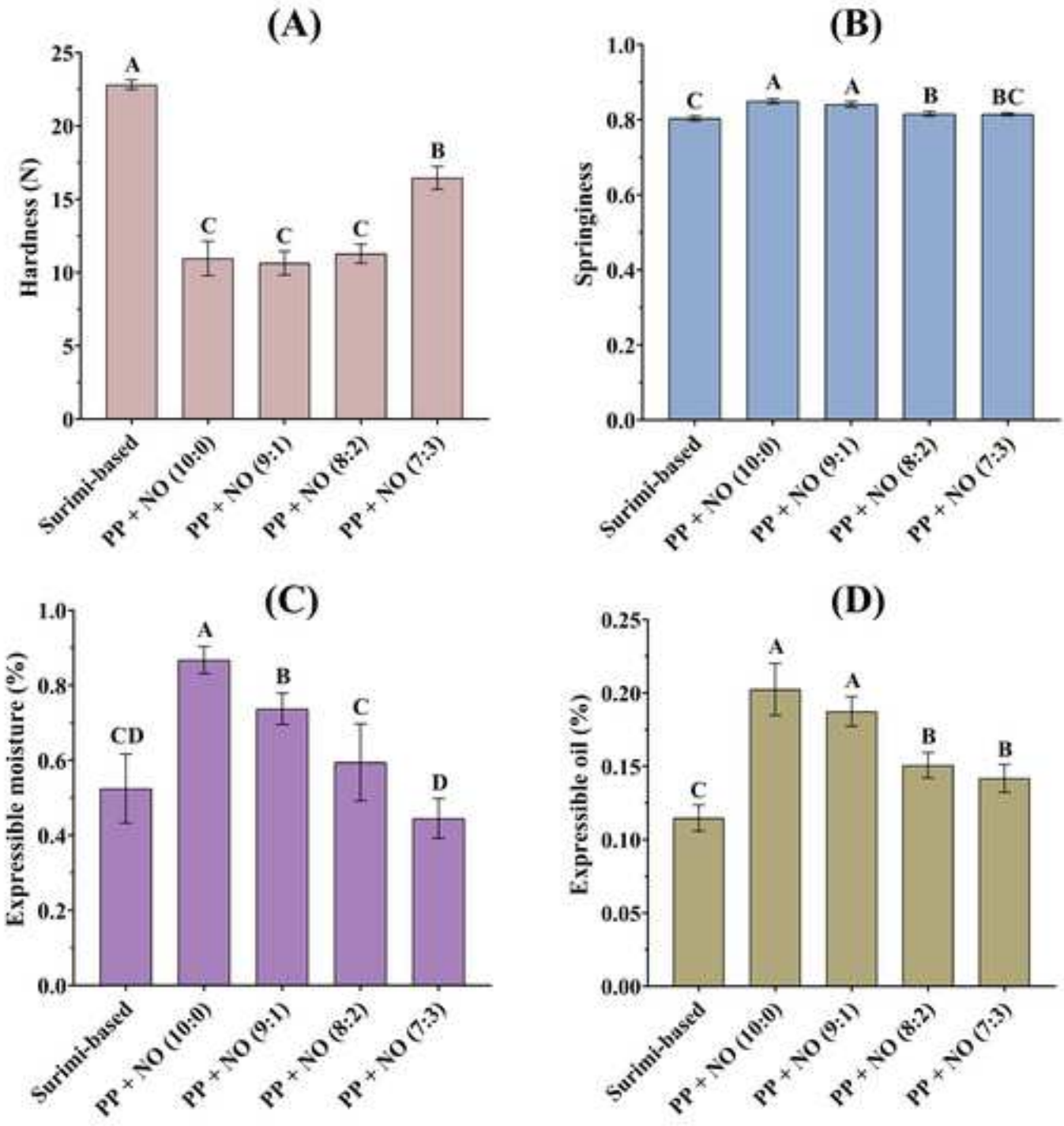
(A)
Hardness (N)
25
20
15
10
5
0
A
C
C
C
B
Surimi-based
PP + NO (10:0)
PP + NO (9:1)
PP + NO (8:2)
PP + NO (7:3)
(B)
Springiness
1.0
0.8
0.6
0.4
0.2
0.0
C
A
A
B
BC
Surimi-based
PP + NO (10:0)
PP + NO (9:1)
PP + NO (8:2)
PP + NO (7:3)
(C)
Expressible moisture (%)
1.0
0.8
0.6
0.4
0.2
0.0
CD
A
B
C
D
Surimi-based
PP + NO (10:0)
PP + NO (9:1)
PP + NO (8:2)
PP + NO (7:3)
(D)
Expressible oil (%)
0.25
0.20
0.15
0.10
0.05
0.00
C
A
A
B
B
Surimi-based
PP + NO (10:0)
PP + NO (9:1)
PP + NO (8:2)
PP + NO (7:3)

Figure 2

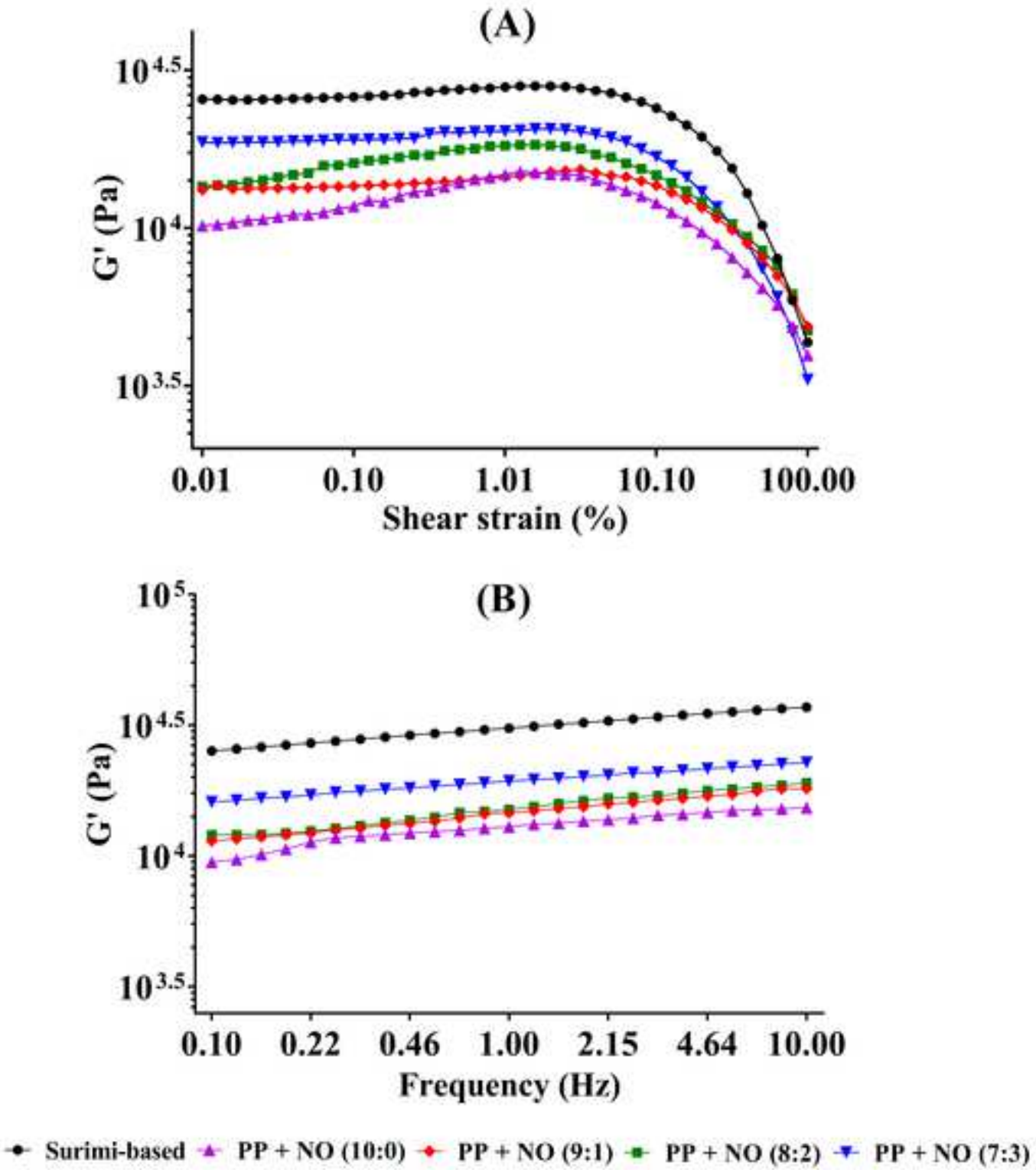
(A)
$10^{4.5}$
10^{4}
$10^{3.5}$
G' (Pa)
0.01
0.10
1.01
10.10
100.00
Shear strain (%)
(B)
10^{5}
$10^{4.5}$
10^{4}
$10^{3.5}$
G' (Pa)
0.10
0.22
0.46
1.00
2.15
4.64
10.00
Frequency (Hz)
Surimi-based
PP + NO (10:0)
PP + NO (9:1)
PP + NO (8:2)
PP + NO (7:3)

Figure 3

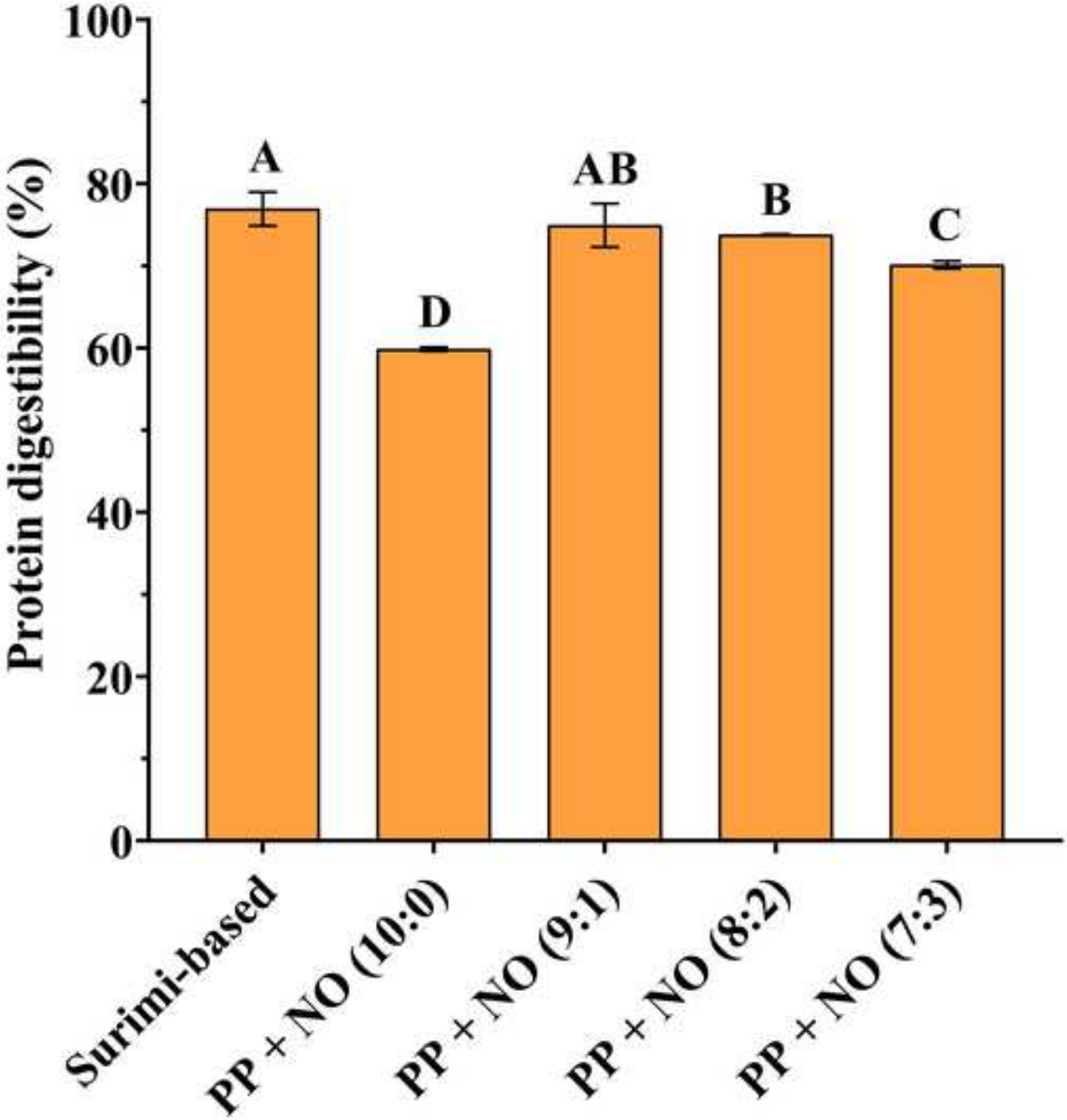
Protein digestibility (%)
100
80
60
40
20
0
A
D
AB
B
C
Surimi-based
PP + NO (10:0)
PP + NO (9:1)
PP + NO (8:2)
PP + NO (7:3)

Figure 4

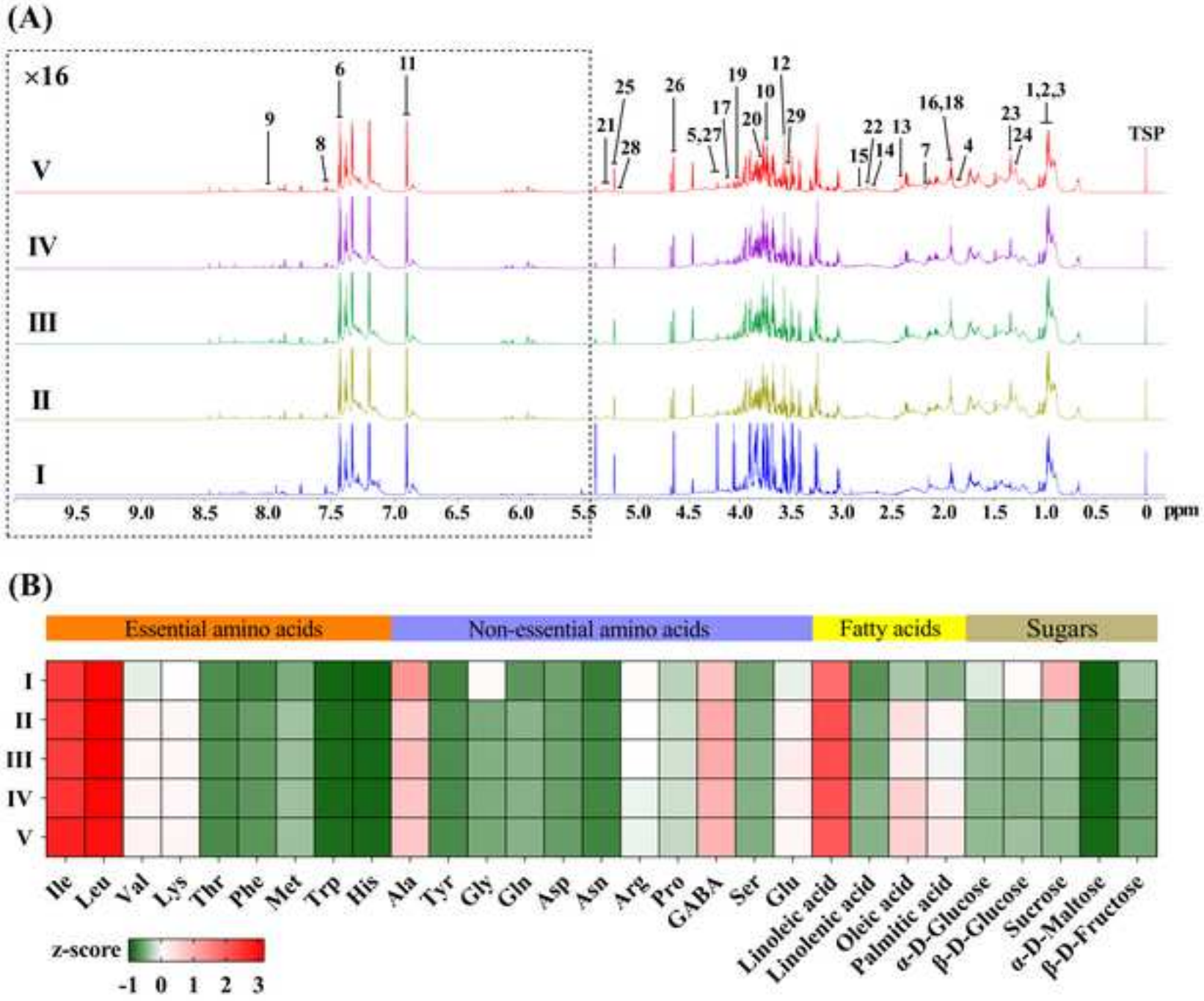
(A)
×16
V
IV
III
II
I
9
8
6
11
21
25
28
26
5,27
17
19
20
10
12
29
15
22
14
13
7
16,18
4
23
24
1,2,3
TSP
9.5 9.0 8.5 8.0 7.5 7.0 6.5 6.0 5.5 5.0 4.5 4.0 3.5 3.0 2.5 2.0 1.5 1.0 0.5 0 ppm
(B)
Essential amino acids
Non-essential amino acids
Fatty acids
Sugars
I
II
III
IV
V
Ile Leu Val Lys Thr Phe Met Trp His Ala Tyr Gly Gln Asp Asn Arg Pro GABA Ser Glu Linoleic acid Linolenic acid Oleic acid Palmitic acid α-D-Glucose β-D-Glucose Sucrose α-D-Maltose β-D-Fructose
z-score
-1 0 1 2 3

Figure 5

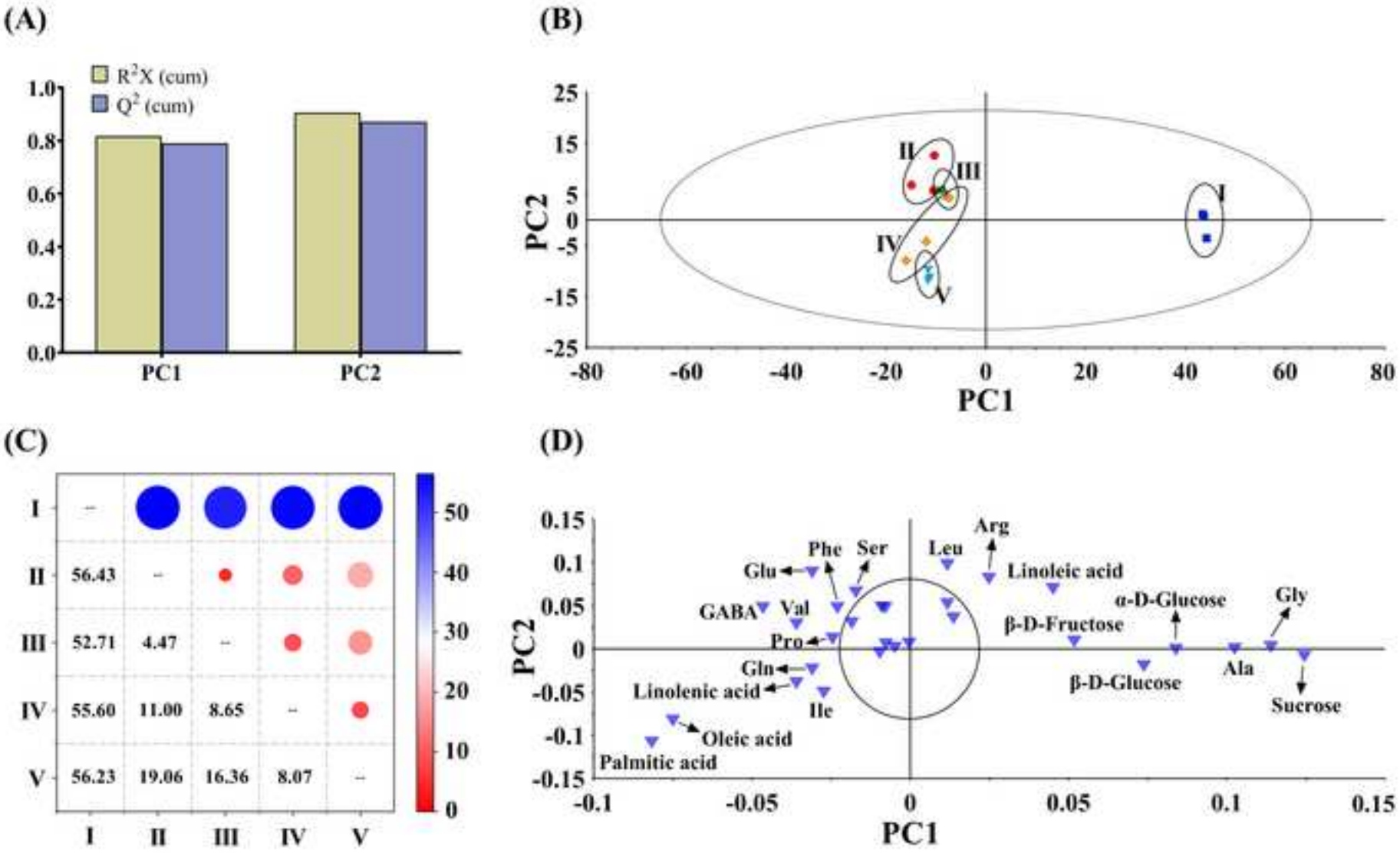
(A)
R²X (cum)
Q² (cum)
1.0
0.8
0.6
0.4
0.2
0.0
PC1
PC2
(B)
25
15
5
0
-5
-15
-25
PC2
-80
-60
-40
-20
0
20
40
60
80
PC1
II
III
I
IV
V
(C)
I
II
III
IV
V
56.43
52.71
4.47
55.60
11.00
8.65
56.23
19.06
16.36
8.07
50
40
30
20
10
0
(D)
0.15
0.1
0.05
0
-0.05
-0.1
-0.15
PC2
-0.1
-0.05
0
0.05
0.1
0.15
PC1
Arg
Phe
Ser
Leu
Glu
Linoleic acid
GABA
Val
α-D-Glucose
Gly
β-D-Fructose
Pro
Gln
Ala
Linolenic acid
β-D-Glucose
Ile
Sucrose
Oleic acid
Palmitic acid

Figure 6

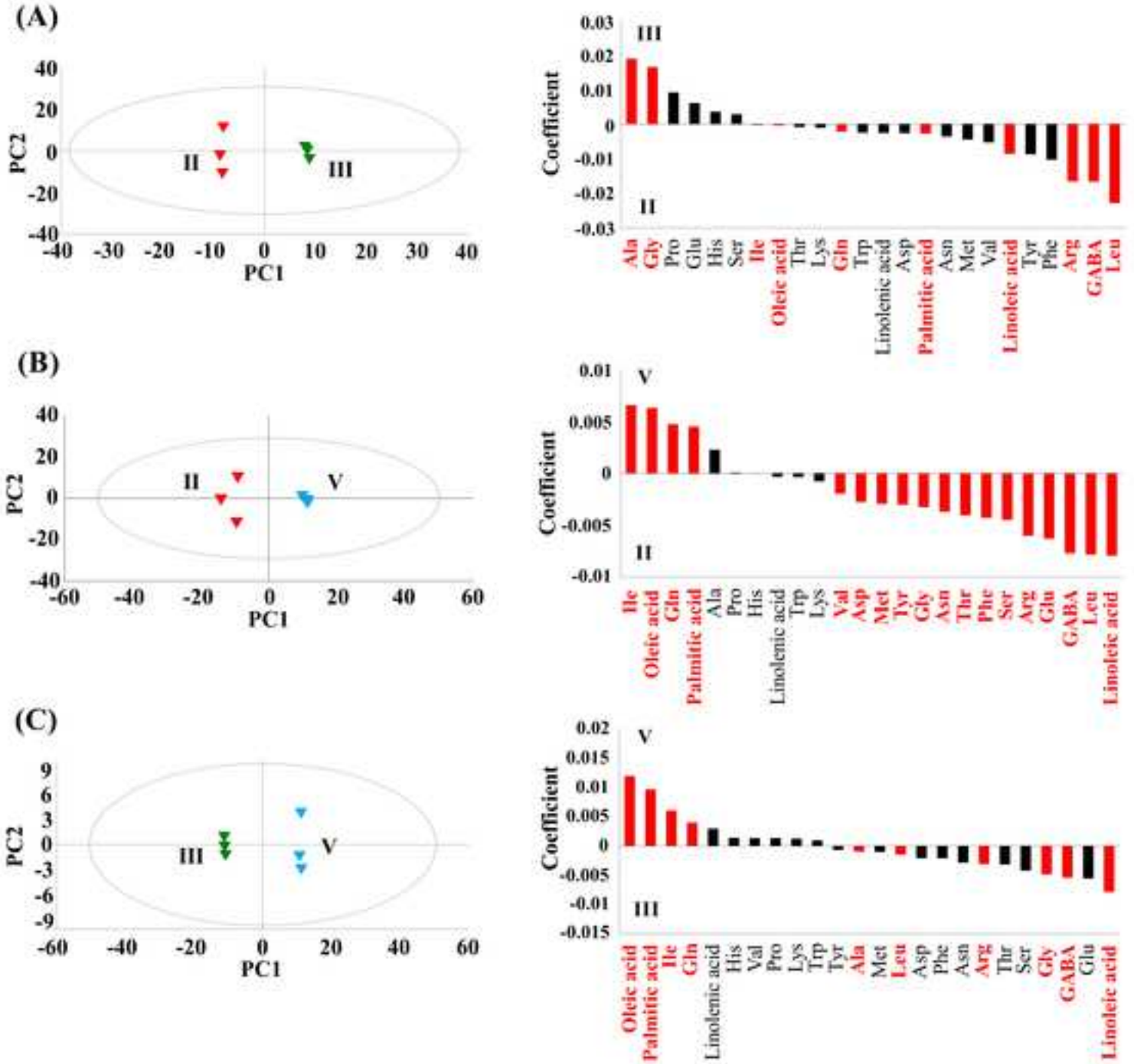

Figure 7

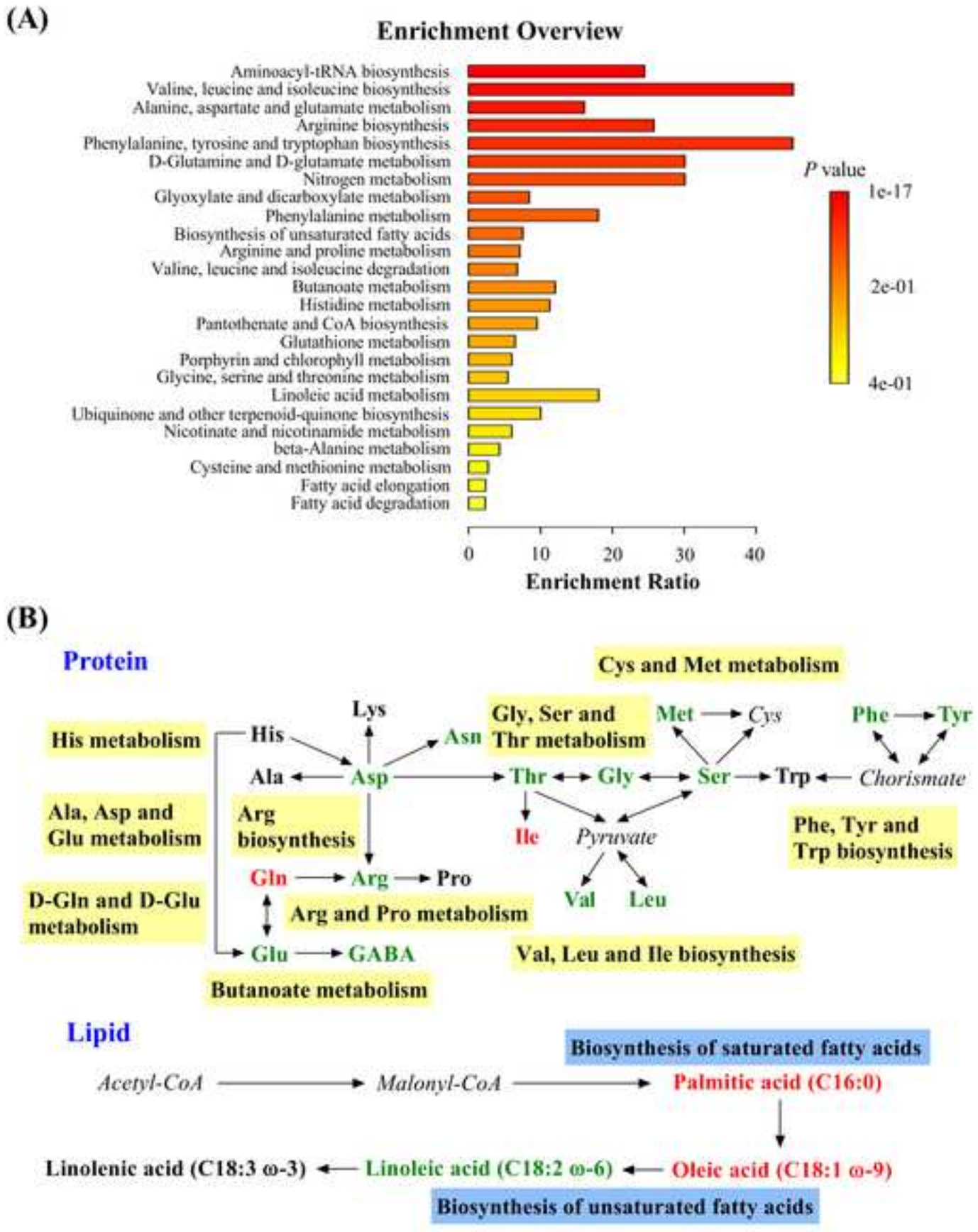
(A)
Enrichment Overview
Aminoacyl-tRNA biosynthesis
Valine, leucine and isoleucine biosynthesis
Alanine, aspartate and glutamate metabolism
Arginine biosynthesis
Phenylalanine, tyrosine and tryptophan biosynthesis
D-Glutamine and D-glutamate metabolism
Nitrogen metabolism
Glyoxylate and dicarboxylate metabolism
Phenylalanine metabolism
Biosynthesis of unsaturated fatty acids
Arginine and proline metabolism
Valine, leucine and isoleucine degradation
Butanoate metabolism
Histidine metabolism
Pantothenate and CoA biosynthesis
Glutathione metabolism
Porphyrin and chlorophyll metabolism
Glycine, serine and threonine metabolism
Linoleic acid metabolism
Ubiquinone and other terpenoid-quinone biosynthesis
Nicotinate and nicotinamide metabolism
beta-Alanine metabolism
Cysteine and methionine metabolism
Fatty acid elongation
Fatty acid degradation
P value
1e-17
2e-01
4e-01
0
10
20
30
40
Enrichment Ratio
(B)
Protein
Cys and Met metabolism
His metabolism
Lys
His
Asn
Gly, Ser and Thr metabolism
Met
Cys
Phe
Tyr
Ala
Asp
Thr
Gly
Ser
Trp
Chorismate
Ala, Asp and Glu metabolism
Arg biosynthesis
Ile
Pyruvate
Phe, Tyr and Trp biosynthesis
Gln
Arg
Pro
D-Gln and D-Glu metabolism
Arg and Pro metabolism
Val
Leu
Glu
GABA
Val, Leu and Ile biosynthesis
Butanoate metabolism
Lipid
Biosynthesis of saturated fatty acids
Acetyl-CoA
Malonyl-CoA
Palmitic acid (C16:0)
Linolenic acid (C18:3 ω-3)
Linoleic acid (C18:2 ω-6)
Oleic acid (C18:1 ω-9)
Biosynthesis of unsaturated fatty acids

Figure 8